REVIEW OPEN ACCESS

Journal of
Venomous Animals and Toxins
including Tropical Diseases

ISSN 1678-9199

www.jvat.org

Electrophysiological evaluation of the effect of peptide toxins on voltage-gated ion channels: a scoping review on theoretical and methodological aspects with focus on the Central and South American experience

Jessica Rojas-Palomino[1&], Alejandro Gómez-Restrepo[2&], Cristian Salinas-Restrepo[3], César Segura[4], Marco A. Giraldo[1], Juan C. Calderón[2*]

[1]Biophysics Group, Institute of Physics, University of Antioquia, Medellín, Colombia.
[2]Physiology and Biochemistry Research Group –PHYSIS, Faculty of Medicine, University of Antioquia, Medellín, Colombia.
[3]Toxinology, Therapeutic and Food Alternatives Research Group, Faculty of Pharmaceutical and Food Sciences, University of Antioquia, Medellín, Colombia.
[4]Malaria Group, Faculty of Medicine, University of Antioquia, Medellín, Colombia.

Keywords:
Patch-clamp techniques
Cellular model
Excitable cell
Venoms
Ionic current
Calcium channels
Potassium channels

Abstract

The effect of peptide toxins on voltage-gated ion channels can be reliably assessed using electrophysiological assays, such as the patch-clamp technique. However, much of the toxinological research done in Central and South America aims at purifying and characterizing biochemical properties of the toxins of vegetal or animal origin, lacking electrophysiological approaches. This may happen due to technical and infrastructure limitations or because researchers are unfamiliar with the techniques and cellular models that can be used to gain information about the effect of a molecule on ion channels. Given the potential interest of many research groups in the highly biodiverse region of Central and South America, we reviewed the most relevant conceptual and methodological developments required to implement the evaluation of the effect of peptide toxins on mammalian voltage-gated ion channels using patch-clamp. For that, we searched MEDLINE/PubMed and SciELO databases with different combinations of these descriptors: "electrophysiology", "patch-clamp techniques", "Ca^{2+} channels", "K^{+} channels", "cnidarian venoms", "cone snail venoms", "scorpion venoms", "spider venoms", "snake venoms", "cardiac myocytes", "dorsal root ganglia", and summarized the literature as a scoping review. First, we present the basics and recent advances in mammalian voltage-gated ion channel's structure and function and update the most important animal sources of channel-modulating toxins (e.g. cnidarian and cone snails, scorpions, spiders, and snakes), highlighting the properties of toxins electrophysiologically characterized in Central and South America. Finally, we describe

*** Correspondence:** jcalderonv00@yahoo.com
[&]These authors contributed equally to this work
https://doi.org/10.1590/1678-9199-JVATITD-2023-0048
Received: 09 October 2023; Accepted: 02 May 2024; Published online: 02 September 2024

the local experience in implementing the patch-clamp technique using two models of excitable cells, as well as the participation in characterizing new modulators of ion channels derived from the venom of a local spider, a toxins' source less studied with electrophysiological techniques. Fostering the implementation of electrophysiological methods in more laboratories in the region will strengthen our capabilities in many fields, such as toxinology, toxicology, pharmacology, natural products, biophysics, biomedicine, and bioengineering.

Background

Cellular electrophysiology allows for the study of the electrical properties of mammalian cells, either non-excitable or excitable. These properties arise from the interplay of several mechanisms: the specific chemical composition of the biological membranes, the differential distribution of ions such as Ca^{2+}, K^+, Na^+, and Cl^- across the cell membranes, and the presence of ion channels in those membranes. A reliable measure of the function of such ion channels became possible only until the development of the patch-clamp technique in the late 1970s and early 1980s by Neher and Sakmann [1–3].

On the other hand, an important number of laboratories were created during the last two decades in Central and South America focused on studies of natural products of vegetal and animal origin. However, even when natural products are gold mines to find regulators on ion channels, most studies in the field lacked complementary electrophysiological approaches. In a few cases, the new molecules were characterized in North America or Europe. Besides infrastructure limitations, this likely happens because researchers are unfamiliar with the scope of the electrophysiological techniques and their suitable cellular models.

Given the potential interest of many research groups in the highly biodiverse region that constitutes Central and South America, here we review the most relevant conceptual and methodological developments of the synergy produced by the study of natural products with an electrophysiological approach. Classical and novel information about the voltage-gated ion channel's structure and function is presented, as well as an update of the most important mammalian voltage-gated ion channel-modulating toxins from animal sources (e.g. cnidarian and cone snails, scorpions, spiders, and snakes), highlighting the channel-interacting toxins described in Central and South America. Then, we explain the local experience of implementing electrophysiological techniques in experimental models of excitable cells, and the participation in screening natural products from animals (venoms, fractions, or toxins) and characterizing new modulators of ion channels. For the latter, we present an instructive, innovative study case of a toxin from a local spider, something uncommon in a region that has focused on scorpion toxins. These developments are expected to strengthen the capabilities of the region in fields like pharmacology, toxicology, toxinology, natural products, biophysics, biomedicine, and bioengineering.

Methods

This scoping review summarizes conceptual and methodological relevant information retrieved from MEDLINE/PubMed and SciELO databases. The search was performed with different combinations of the following descriptors: "electrophysiology", "patch-clamp techniques", "Ca^{2+} channels", "K^+ channels", "cnidarian venoms", "cone snail venoms", "scorpion venoms", "spider venoms", "snake venoms", "cardiac myocytes", and "dorsal root ganglia", with no language or year constraints. For the sake of clarity and conciseness, because of the lack of Central and South American literature on other channels, and real future potential practical applications in laboratories of the region, we did not extend the review to other channels or cellular experimental models.

The titles of all original papers retrieved until September 2023 were screened independently by two researchers and deemed eligible if they seemed to present novel experimental information on the structure of voltage-gated Ca^{2+} and K^+ channels, described the effect of one or more peptide toxins on mammalian voltage-gated Ca^{2+} and K^+ channels using electrophysiological techniques or detailed a patch-clamp protocol for studying peptide toxins on cardiac myocytes or dorsal root ganglia. A further refinement was then performed to identify non-redundant examples of the most important mammalian voltage-gated interacting toxins from cnidarian and cone snails, scorpion, spider, and snake sources, as well as the literature with key participation of research laboratories from Central or South America, between 1996 and 2023.

The quality of the papers was judged according to the quality of writing and reporting of their results, use of appropriate statistical approaches, number of experiments performed (including controls), and coherence among the objectives, methods used and conclusions reached. Finally, a few documents in languages other than English or Spanish were removed. The reporting of results of the present work follows the Preferred Reporting Items for Systematic Reviews and Meta-Analyses Extension for Scoping Reviews (PRISMA-ScR) guidelines [4]. Figure 1 presents a flow diagram with the process of selection of the sources of evidence.

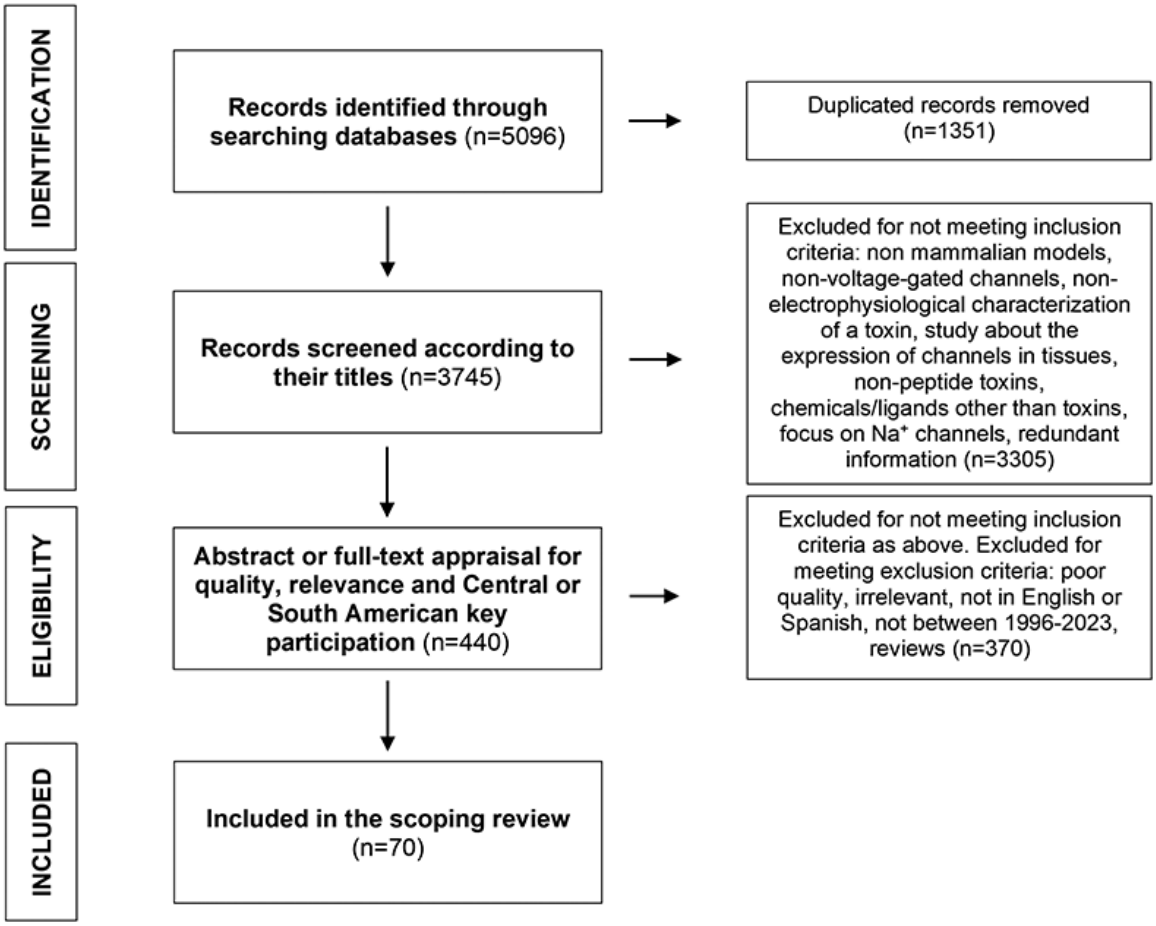

Figure 1. Flow diagram with the process of selection of the sources of evidence.

Conceptual aspects

Ca^{2+} and K^+ channels in excitable cells

Excitable cells can develop and conduct action potentials (AP), i.e., rapid changes in the potential difference across the membrane, as a response to a stimulus (e.g., mechanical, electrical or chemical). This property mediates the communication between cells and participates in multiple regulatory processes involving intracellular metabolism, signal transduction, sensing the environment, learning, gene expression, secretion of hormones, muscle contraction, and protein degradation, among others [5]. The main molecular mechanism underlying this property is the transport of ions in a concerted fashion through voltage-gated ion channels [6]. These channels are enriched in the membrane of the excitable cells, such as neurons and muscle cells, but are also present in some cells with negative resting membrane potentials, but which do not fire AP, such as the immune cells [5,7].

Ion channels have one of two typical structures, either a large, monomeric α-subunit or a polymeric α-subunit composed of smaller subunits. Voltage-gated Ca^{2+} channels represent the first structure and voltage-gated K^+ channels are the prototype of the second.

Voltage-gated Ca^{2+} channels (Ca_v)

Changes in the cell membrane potential (V_m) activate Ca_v, leading to a Ca^{2+} influx, in turn involved in the regulation of many physiological processes, such as the release of neurotransmitters in neurons, the contraction of cardiomyocytes, or the sarcoplasmic Ca^{2+} release in skeletal muscle [8,9]. These channels are composed of one α-subunit, and several accessory subunits, as recently confirmed by cryoelectron microscopy reconstructions done with a resolution below 3.6 Å [10,11]. The α-subunit (Figure 2A) consists of a monomer with four homologous domains (DI–DIV) and is the principal component of the channels because it has the transmembrane pore domain (PD) and the voltage sensing domain (VSD) [9]. Each homologous domain contains six transmembrane α-helices (S1-S6) with a membrane-reentrant loop between them and cytoplasmic regions at the N and C terminal ends. The S5 and S6 helices constitute the PD and the S4 is the voltage-sensing helix of the VSD (S1-S4). The pore creates a permeation path for Ca^{2+} and crosses from the negatively charged dome region, which faces the extracellular space, to the intracellular space. The narrowest part of this permeation path is known as the selectivity filter (SF). The external region of the SF contains a couple of glutamate residues in each domain,

which are required for Ca^{2+} ions selectivity. Each S6 forms the internal region of the SF from DI-DIV and constitutes a binding site for some Ca^{2+} antagonists, such as diltiazem and verapamil [10–12]. The S4 consists of repeated motifs of positively charged residues arginine and lysine, followed by two hydrophobic residues. During depolarization, the S4 moves towards the extracellular space, producing a conformational change in the PD and allowing the passage of ions. The inactivation gate is the loop linker between DIII-S6 and DIV-S1. Accessory subunits β, γ and $\alpha_2\delta$ modify biophysical and pharmacological properties besides influencing the abundance and trafficking of Ca_v channels [9,13] (Figure 2A).

Three major subfamilies of Ca_v, Ca_v1, Ca_v2, and Ca_v3 [9,14,15], underlie the existence of six different types of Ca^{2+} currents (L-, N-, P-, Q-, R-, and T-type). $Ca_v1.1$, $Ca_v1.2$, $Ca_v1.3$, and $Ca_v1.4$ have been cloned for the L-type Ca^{2+} current (I_{CaL}, L stands for large conductance and long openings). They are activated from about -30 mV and are highly sensitive to dihydropyridines (DHP) [16]. $Ca_v1.1$ is expressed in the skeletal muscle, while $Ca_v1.2$ and $Ca_v1.3$ are in the heart and neurons. $Ca_v1.4$ expression is major in the retina, spinal cord, and immune cells. $Ca_v2.1$ (P/Q-type, $I_{CaP/Q}$), $Ca_v2.2$ (N-type, I_{CaN}), and $Ca_v2.3$ (R-type, I_{CaR}) are expressed in neurons of the cerebellum, brain, and peripheral nervous system [12]. Three genes *(CACNA1G, CACNA1H*, *CACNA1I*) encode for channels $Ca_v3.1$, $Ca_v3.2$, and $Ca_v3.3$, responsible for the T-type currents ($I_{CaT,}$ tiny currents, almost insensible to DHP, that activate at more negative potentials, i.e. –70 to –40 mV, and inactivate fast) [16]. $Ca_v3.2$ is expressed in embryonic heart tissue. In adults, $Ca_v3.1$ expression is higher than $Ca_v3.2$ [16]. Given its expression, these channels are targets for the treatment of pain, stroke, epilepsy, migraine, and hypertension [17].

Voltage-gated K^+ channels (K_v)

K_v is by far the largest and most diverse family of ion channels and underlies a large number of K^+ currents (I_K) with different kinetics. They are largely responsible for the repolarization phase of the AP and are important in signal transduction, immunity, and blood pressure [7,18–20]. Structurally, their α-subunit is composed of individual monomeric, not necessarily identical, subunits (DI to DIV), which assemble within the membrane. Each monomeric domain contributes with the S5 and S6 to build a pore (PD) down their center (Figure 2B), while S4 works as the voltage-sensing helix of the VSD. The SF in the PD is formed by oxygens from the lateral chains of threonine (T) and the

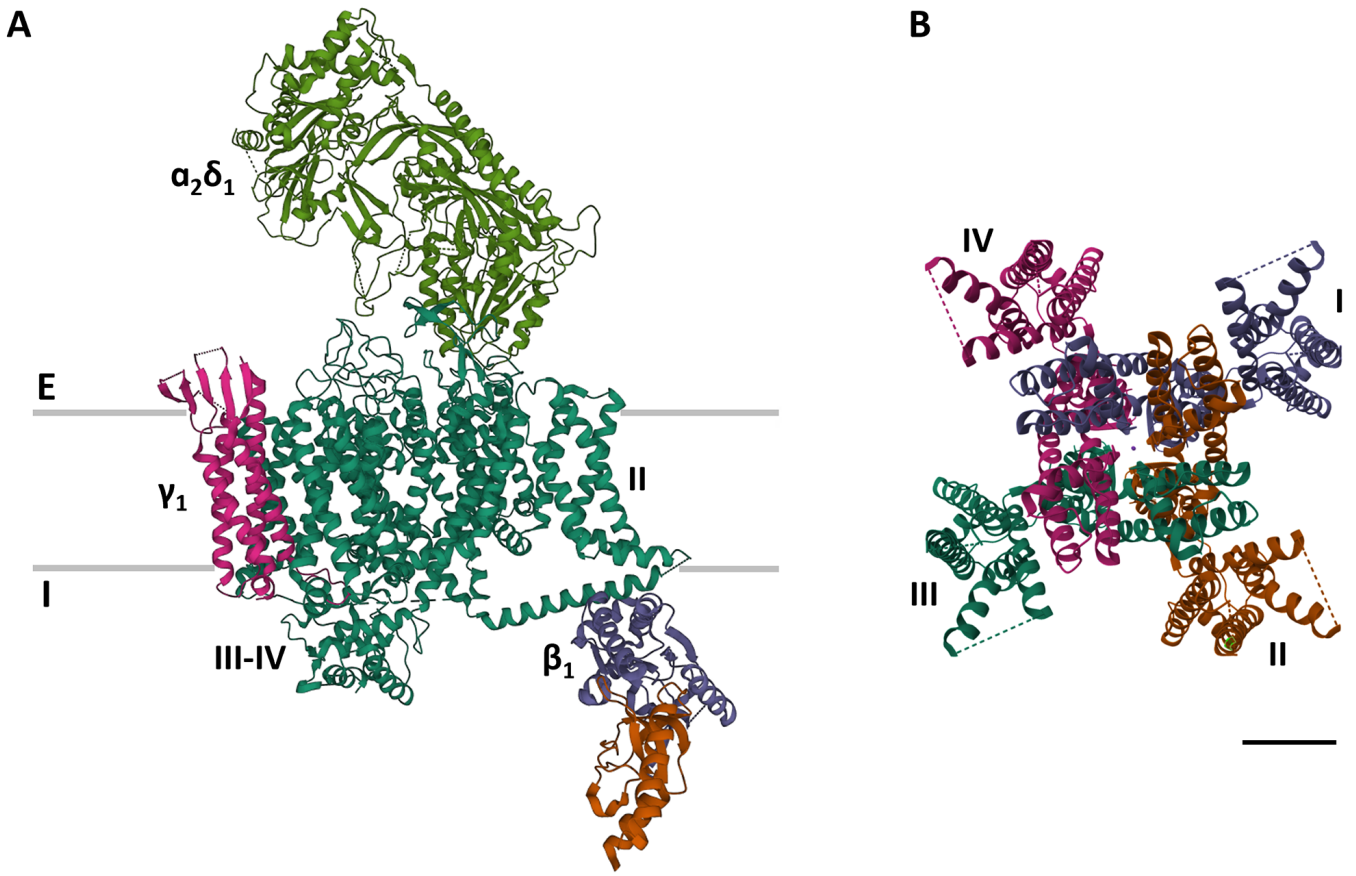

Figure 2. Structure of voltage-gated Ca^{2+} and K^+ channels. **(A)** Lateral view of the structure of the mammalian voltage-gated $Ca_v1.1$ complex. Gray lines represent the exterior (E) and interior (I) boundaries of the cellular membrane. II and III-IV indicate domains of the homologous α-subunit (green). Other subunits ($\alpha_2\delta_1$, γ_1, β_1) are also indicated. **(B)** Top view of the voltage-gated $K_v1.3$ channel, showing the pore in the center. I to IV indicate the monomeric α-subunits. Structures taken from the Protein Data Bank (rscb.org), IDs: 5GJV and 7SSX, for $Ca_v1.1$ and $K_v1.3$, respectively. Calibration bar: 2 nm.

residues glycine (G) and tyrosine (Y), in a TXGYG sequence, where X represents a variable residue (usually valine (V) or isoleucine (I)). Like in the Ca_v, the VSD is equipped with about five positively charged amino acids (arginine or lysine) at every third position. Depending on the direction and magnitude of the electric field, the VSD conformation changes, leading to the pore's opening [21–25]. The mechanism of K^+ conduction in its SF has been elucidated by molecular dynamics and the knowledge of its structure through X-ray diffraction of the KcsA channel [25,26].

In mammalian genomes, the α-subunits of the K_v channels are encoded by 40 different genes, classified into 12 distinct subfamilies. *Shakers* (K_v1.1 to K_v1.8), are expressed in the nervous system, heart, skeletal and smooth muscle, pancreas, lung, placenta, kidney, retina, colon, and T cells. *Shabs* (K_v2.1 and K_v2.2), are present in the brain, heart, neurons, and smooth muscle. *Shaws* (K_v3.1 to K_v3.4), are located in skeletal muscle, pancreas, liver, and lymphocytes. *Shals* (K_v4.1 to K_v4.3), are present in the brain, heart, smooth muscle, and neurons. *KCNQ* (K_v7.1 to K_v7.5) family is expressed in the nervous system, heart, pancreas, ear, kidney, lung, colon, placenta, and skeletal muscle. Ether-a-go-go related gene –*ERG*– (K_v10.1, K_v10.2, K_v11.1, K_v11.3, K_v12.1, K_v12.3) channels are generally found in the central nervous system and heart [15,18,22].

A fascinating characteristic of the K_v channels is their functional diversity, as manifested in a very variable spectrum of I_K kinetics. This can be explained in part because of the existence of structural differences among the large number of α-subunit isoforms mentioned above. However, another explanation includes the presence of a sizeable number of families and isoforms of auxiliary subunits, which regulate the intracellular trafficking, membrane location, voltage dependency, and inactivation of the K_v channels. These auxiliary subunits include K_vβ, KChAP (K_v channel-associated protein), KChIP (K_v channel-interacting protein), KCNE (K^+ voltage-gated channel subfamily E regulatory subunit), and DPPX (Dipeptidyl-aminopeptidase-like protein 6) [5,23,27,28]. A complex relationship between α- and auxiliary subunits creates many possible functional channels with one α-subunit and one or more auxiliary subunits, as it has been brightly demonstrated for instance for the K_v7.1/KCNE1/KCNE3, K_v7.1/KCNE1/KCNE4, and K_v7.1/KCNE3/KCNE4 heteromeric complexes [29]. Moreover, monomers of α-subunits of some isoforms may ensemble with monomers of other α-subunit isoforms in heteromeric functional channels which may have membrane locations and biophysical properties different from their mother isoforms, as it has been shown for K_v1.4/K_v1.6/KCNE channels in experimental models of channels expression, for K_v7.1/K_v7.5 in smooth muscle cells and for K_v4.2/K_v4.3/KChIP2 heteromeric complexes in murine cardiomyocytes [30–32].

K_v and Ca_v have essentially the same states, controlled by the transmembrane potential [5,33]. The opening of the gate (activation) is triggered by the membrane depolarization that energetically favors a continuous water-filled pathway where channels selectively discriminate which ions pass across the membrane. Subsequently, and even when the depolarization stimulus persists, the channels become inactivated. It means that the S4 helix stays in the "up" configuration, while the pore is still in the *open* conformation, but in a nonconducting state. Upon membrane repolarization, i.e., when the stimulus is removed, the channels are *deactivated*, acquiring the *closed* configuration [34].

Voltage-gated ion channels are one of the best-studied types of transmembrane proteins, in part because of the availability of a powerful tool: patch-clamp. This electrophysiological technique has led to a wealth of knowledge about the nature of the biophysical and physiological mechanisms of channel gating. Besides, patch-clamp allows to study the channels as targets of natural or synthetic pharmacological regulators.

The patch-clamp technique

In the late 1970s, recordings of channel currents flowing across the membrane were performed for the first time by Sakmann and Neher [2]. While improving the method, the possible applications of the patch-clamp technique to study ion channels in many cell types were clear [1]. Both researchers were thus awarded the Nobel Prize in Physiology or Medicine in 1991 [35]. Currently, patch-clamp is the gold standard for studying ion channel currents, because it offers quantitative information about the relationship between the transmembrane potential and the ion movement in living cells [36].

A conventional patch-clamp setup requires a system for mechanical and electromagnetic isolation, a magnifying system for visualization of the preparation, a stage and an experimental chamber suitable for the cellular models, equipment to fabricate the micropipettes, a micromanipulator, the electrical amplifier system, a digitizer and software, and hardware adequate for signal acquisition and processing (see section "I_{Ca} and I_K studies").

The technique starts by establishing physical contact with a cell membrane using a glass micropipette filled with an electrolytic solution and a recording electrode (then becoming a microelectrode). The solution inside the micropipette typically resembles the composition of the intracellular milieu. Once the contact is established, a gentle suction is applied through the microelectrode, and a part of the membrane is suctioned into the pipette, with the subsequent increase of the electrical resistance. If done properly, a mechanically stable, high-impedance 'gigaseal' (> 1 GΩ) is established [1]. The gigaseal is key to increasing the signal-to-noise ratio (SNR) of the current signal. Starting from the gigaseal formation (cell-attached configuration), different configurations can be achieved [1,36–39].

If the patch membrane is ruptured, the whole-cell configuration is obtained. This configuration is particularly important and the most frequently used because direct contact between the cell's cytoplasm and the micropipette's internal solution is created. It allows for the study of the total (so-called macroscopic) membrane ionic currents and the AP, depending on the recording mode, voltage-clamp, or current-clamp, respectively [36–40].

A second, reference (also known as ground) electrode is placed in the bath solution (external to the cells) to complete the circuit. The composition of the bath solution resembles that of the extracellular medium.

The circuitry for voltage-clamping the cell membrane is particularly important for the success of the experiments. In a typical whole-cell, voltage-clamp experiment, a command potential (V_c) generated by the amplifier system is imposed for a defined period (usually between 100 ms and 2 s) to the microelectrode, which is in turn expected to be transferred to the cell membrane so that $V_m = V_c$. To do so, the device is equipped with a negative feedback function that rapidly and continuously compares V_m with V_c and if different, injects current. As long as the membrane seal resistance remains high, V_c and V_m become virtually identical in a few microseconds. This procedure is repeated to sequentially clamp V_m at different voltages in steps which are typically of 10 mV, in the so-called voltage-clamp protocol [36–39].

As stated, V_m is responsible for the conformational change of the VSD of the studied channels [5], therefore the different voltage-clamp steps lead to the graded opening of the channels. The consequent reduction of the membrane resistance to the ions creates a flow of ions (i.e., movement of charges), measurable as an ionic current, I_x. The total current, I_t, flowing through the membrane is the sum of all the ionic currents I_x and the capacitive current, I_C:

$$I_t = I_C + \sum I_x \quad (1)$$

I_C depends on the membrane capacitance (C_m):

$$C_m = \varepsilon \frac{A}{d} \quad (2)$$

Where ε is the dielectric constant, A is the membrane area, which changes according to the cell size, and *d* is the membrane thickness, which can be considered constant.

Since the current flowing through the channels may change V_m, an extra amount of current is then injected by the system through the microelectrode so V_m does not diverge from V_c during the voltage step. The magnitude of the extra current injected serves as a measure of the current flowing through the microelectrode and thus through the ion channels present in the membrane so that I_x is reported by the patch-clamp device for each voltage step [36–39]. The magnitude of I_x depends on the conductance of the ion (g_x) and the difference between V_m and the reversal potential of the ion, V_x:

$$I_x = g_x(V_m - V_x) \quad (3)$$

The values of I_x are usually normalized to the C_m (also given by the device) to correct for cell size and the number of functional α-subunits in the cell membrane [38]. The units of this current density are thus A/F (Ampere/Farad), but generally presented as pA/pF (picoAmpere/picoFarad), which will be identical in value.

Once in the open state, each channel displays a unitary single-channel conductance, *g*. The macroscopic conductance, G, of the channels in a membrane, is the ratio of I_x to the external voltage imposed at each voltage step of the current to voltage (I–V) plot [37,41]. Thus, G is the product of the total number of opened channels. The channel-open probability is the normalized macroscopic conductance to its maximum value (G/G_{max}) [37,42].

Reducing electronic noise in cell electrophysiology is crucial. In patch-clamp, the largest individual noise may dominate total noise. This is a consequence of the fact that most of the noises in this technique are uncorrelated, which allows the expression of the total root mean square (RMS) noise as the square root of the sum of the individual squared RMS noise ($e_T^2 = e_1^2 + e_2^2 + e_3^2 ...$) sources) [43]. Background noise arises from a variety of sources: Johnson's noise of the membrane-seal combination, the "shot noise" from ions crossing the membrane, intrinsic noise in the pipette, and the noise in the current-to-voltage converter and capacitance's transients [1,37]. Noise can be largely controlled by grounding the setup, using a system for electromagnetic isolation, avoiding high temperatures during experimentation, ensuring high-resistance seals, and low-pass filtering the signals. Series resistance compensation (Rs), capacitance transient cancellation, and whole-cell compensations have been developed to reduce some types of noise sources and improve the quality of voltage-clamping so that the voltage control is optimal and the SNR can be the largest possible [1,43–45].

Besides recording macroscopic currents, the patch-clamp technique permits the study of the effects of toxins on single-channel kinetics. This can be accomplished with cell-attached, inside-out, or outside-out configurations [1,36–39,46]. Cell-attached have the advantage of allowing to perform single-channel recordings without exchanging the content of the microelectrode with the cytosol, hence avoiding any biochemical disturbances in the intracellular milieu. These high-resistance approaches permit the investigation of the gating properties of an individual or a few channels (usually up to two or three) under the effect, for instance, of different ligands. The signals can be analyzed for open and closed time durations and offer information about the conductance of the channels.

It is worth mentioning that manual and automated patch-clamp are complementary techniques. The latter has recently emerged as a high-throughput screening approach to study the effect of toxins on different ion channel isoforms [47].

Two-electrodes voltage-clamp is another electrophysiological method in which one electrode is focused on measuring the V_m and the other is destined to inject current. This improves the voltage control mainly when performing experiments in large cells, more reliably tracking the open and close kinetics of the channels when evaluating the effect of toxins [48–51].

Whatever the configuration or the number of electrodes used, obtaining a good signal depends on the quality and resolution of the equipment used in the setup and the technical skills of

the researchers. In any case, patch-clamp is an invaluable tool in studying ion channels [1,37]. In our laboratory (see section "I_{Ca} and I_K studies"), the cutting-edge electronic components possess sufficient resolution to record currents for long-term experiments, with low noise.

Why do we study animal toxins with electrophysiological techniques?

General concepts

Animal venoms are mixtures of different types of biomolecules that include proteins, peptides, amino acids, neurotransmitters, and salts, which alter physiological processes in the inoculated animal. Toxins are the main active compounds of venoms, which are widespread among invertebrate and vertebrate phyla [52–54]. Peptide toxins that interact with ion channels are typically made of 10-45 amino acids in invertebrates from the Cnidaria phyla and the Conidae family, namely the cone snails. In invertebrates of the Arthropoda phyla, such as the scorpions and spiders, and vertebrates of the Reptilia class, such as the snakes, most toxins are of up to 75 amino acids. All these toxins are characterized by a low molecular weight (< 10 kDa) and one to five cysteine bridges [18,55–58].

The patterns of distribution of the cysteine residues in the primary sequences generate frameworks which in turn result in particular tridimensional arrangements of α-helices, β-strands, loops, and disulfide bonds that stabilize the structure of the peptides, giving origin to the large, surprising, and complex structural diversity of toxins. The folding patterns originated by the disulfide bonds confer optimal three-dimensional interactions with its target receptor sites, as well as resistance to proteases, high temperatures, pH changes, and harsh chemicals [59,60]. A very large number of tridimensional arrangements have been recognized for invertebrate and vertebrate channel-modulating toxins. For instance, folds A, B, and C (inhibitor cystine knot -ICK- motif) are the most common arrangements in cone snail toxins [56]. Folds A and B are small structures rich in α-helices, while the ICK motifs are formed by two or three strands of β sheets with three disulfide bridges that form a cystine knot [56,60]. The ICK motif is also common in spider and scorpion toxins. Spiders also present the disulfide-directed β-hairpin (DDH) fold and scorpion toxins are rich in the cysteine-stabilized α/β (CSα/β) and cystine-stabilized helix-loop-helix (CSαα) motifs [18,55,57,58,61]. In contrast, snake toxins can form more complex, large structures, including the three-finger toxins (3FTx, enriched in β-strands), cysteine-rich secretory proteins (CRISP, one larger domain rich in α-helices, β-strands and loops connected to a smaller domain rich in α-helices) and BPTI-Kunitz-type (α-helices, β-strands and a long inhibitory loop) peptides [62–64]. Of note, CRISP, for instance, has also been reported in spiders and scorpions, and ICK and CSα/β motifs are also present in snake toxins [63,65], highlighting that most motifs and tridimensional arrangements are not exclusive of any type of venomous animal.

Remarkably, the presence of cystine bridges and the folding patterns favored by them confer toxins the ability to bind and modulate (i.e., activate or inhibit) voltage-gated ion channels with high affinity, being therefore called disulfide bonding, or bridged, peptides (DBP) [66]. This property has been used to understand the role, diversity, structure-function relationship, gating, and tissue localization of ion channels [29,67,68]. For this reason, venoms and toxins are considered gold mines of channel regulators and therapeutic agents with a lot of potential applications [69–73]. Accordingly, several venom-based molecules are successfully used as leads in basic research and drug discovery [74–76], as will be shown in the following section.

Main sources of channel-modulating toxins

Cnidarian and cone snails, scorpions, spiders, and snakes are the main sources of venoms enriched in mammalian voltage-gated ion channel-modulating toxins. For each of them, we present some representative toxins described around the world and then comprehensively present the toxins characterized by Central and South American research groups.

Cnidarian and cone snails: Cnidaria and Mollusca phyla include marine invertebrates particularly enriched in toxins [77,78]. Cnidaria includes five classes and more than 10,000 species of jellyfish, sea anemones, and corals, among others [78]. The genus *Conus* highlights within the Mollusca phylum because it includes over 900 marine species of cone snails [77]. Toxins derived from cnidarians and cone snails target many ionic and non-ionic channels and have shown interesting applications. For example, dalazatide is a potent, selective blocker of $K_v1.3$, derived from the Stichodactyla toxin (ShK) of the venom of the *Stichodactyla helianthus* sea anemone, which is in Phase II clinical trials for the treatment of immune diseases [79]. Similarly, the potent MNT-002 antibody-ShK conjugate has served to better understand the $K_v1.3$ pore-blocking dynamics at atomic resolution, further supporting ShK conjugates' prospective use as immunomodulators [80].

The classification of the large amount of disulfide-rich toxins derived from cone snails is complex, and it has been performed according to their gene superfamily, their cysteine framework, and their pharmacological targets [56,77]. Conotoxins from the A, D, I, J, M, and O gene superfamilies commonly modulate voltage-gated ion channels. MVIIA, MVIIB, MVIIC, and MVIID, from *Conus magus*, target channels of the Ca_v2 family [81]. Ziconotide (a synthetic analog of MVIIA) is now used to treat neuropathic pain [17,82]. Other conotoxins have potential as analgesics by acting on Ca^{2+} channels as well (e.g., FVIA, CVIB, GVIA, Tx6.7, MoVIA, MoVIB, TxVIA) [81,83–85]. The recently investigated Mu8.1 toxin from *Conus mucronatus*, which inhibits $Ca_v2.3$ [47], highlights because it is about twice as large as the majority of conotoxins known to block ion channels. Conotoxins have also provided a variety of toxins specifically acting on some K_v channels. ViTx from *Conus virgo* inhibits $K_v1.1$ and $K_v1.3$, but not $K_v1.2$ or $K_v11.1$ [86], pl14a from *Conus planorbis* selectively blocks $K_v1.6$, but not $K_v1.2$, $K_v1.3$, $K_v1.4$, $K_v1.5$, $Na_v1.2$ or I_{CaN}

[87], and κ–PVIIA from *Conus purpurascens* and κM-RIIIK from *Conus radiatus* inhibit *Shaker* channels [88,89]. Further studies demonstrated that κM-RIIIK and κM-RIIIJ from *Conus radiatus* inhibit K_v1.2, but not K_v1.3, K_v1.4, Kv1.5, K_v7.2 or K_v11.1 [89,90]. Noticeably, the ability of κM-RIIIK to block K_v1.2/K_v7.2 heteromeric channels may confer it cardioprotective properties [90]. Despite the selectivity of many conotoxins, some others (e.g., μ-PIIIA, μ-SIIIA) have been shown to block K_v, but also Na_v isoforms [91].

Only a few studies on cnidarian or cone snail venoms or toxins come from Central or South American laboratories. A Mexican-Argentinian collaboration showed that the complete venom of the Mexican cnidarian *Palythoa caribaeorum* blocks Ca_v2.2 in rat superior cervical ganglion neurons. This venom is enriched in low molecular weight peptides (mostly ~2-4 kDa), however, the isolation of one or more specific toxins responsible for this effect constitutes an avenue for future research [92]. Moreover, two toxins, BcsTx1 and BcsTx2, from the sea anemone *Bunodosoma caissarum* from Brazil have shown the ability to block K_v1.1, K_v1.2, K_v1.3, and K_v1.6 isoforms with very high potency [49].

Although most cone snail species inhabit the African and Asian Ocean Pacific waters, many species are known to be present in the American coasts [77,93]. Mexican, Brazilian, and Cuban efforts have revealed the effect of some conotoxins from American coasts on voltage-gated ion channels. The toxin sr11a from *Conus spurius* blocks K_v1.2 and K_v1.6, but not K_v1.3 [94]. Interestingly, PiVIIA from *Conus princeps* activates I_{Ca} in rat dorsal root ganglion neurons [95]. Many other conotoxins reported by Central and South American groups await electrophysiological characterization [96–98].

Scorpions: The best-studied toxins from the scorpion venoms act by binding to four groups of ion channels in excitable cells [57]: Na_v (NaScTx) [99], Ca_v (CaScTx) [100], K_v (KScTx - α-Ktx, β-Ktx, γ-KTx, δ-KTx, ε-Ktx, κ-KTx, and λ-KTx) [101,102], and Cl_v (ClScTx) [103]. Kurtoxin, isolated from *Parabuthus transvaalicus* inhibits N-type and L-type Ca^{2+} currents in thalamic neurons and slows down current activation kinetics, acting as a gating modifier toxin [104]. This toxin also demonstrated the modulatory capacity of Na_v1.6 currents in the murine *vas deferens* myocytes. This toxin has a dual effect, increasing peak amplitude at potentials between -40 and -30 mV, and decreasing peak amplitude for potentials more positive than -10 mV [105]. Charybdotoxin from the venom of *Leiurus quinquestriatus hebraeus,* Agitoxin2 from *Leiurus quinquestriatus hebraeus,* Ev37 from *Euscorpiops validus*, margatoxin from *Centruroides margaritatus* and HelaTx1 from *Heterometrus laoticus* [106–111], inhibit several isoforms of the Shaker subfamily (K_v1.x) of channels likely by occluding the pore, whereas BmPO5 from the Asian scorpion *Buthus martensii* binds to the K_{Ca}2.2 [112]. Interestingly, venoms of the *Androctonus* genus harbor toxins with opposite effects on K_v. While AmmTx3 from *A. mauretanicus* blocks K_v4.2, AbTXKβ$_{(2-64)}$ from *A. australis* activates K_v7.3 and K_v7.4 isoforms [113,114].

There are four main families of scorpions in Central and South America: Buthidae, Chactidae, Diplocentridae, and Liochelidae. Buthidae, the largest and most studied family, comprises five genera: *Ananteris, Centruroides, Microtityus, Rhopalurus*, and *Tityus* [101,115]. Mexico and Brazil, in collaboration with Hungarian and Belgian scientists, have contributed significantly to the electrophysiological characterization of venoms and toxins from the American scorpions. Notably, the first K^+ channel-blocking peptide identified using voltage-clamp was Noxiustoxin (toxin II.11) [116], a toxin from *Centruroides noxius,* a scorpion of the Buthidae family, native from Mexico. This scorpion also expresses cobatoxins, which block K_v1.1 channels [51]. Many other scorpion toxins isolated from species of America also block K_v1.1, K_v1.2, or K_v1.3 isoforms, such as Pi1, Pi2 and Pi3 from *Pandinus imperator* [117], Tc30 and Tc32 from *Tityus cambridgei* [118], anuroctoxin from *Anuroctonus phaiodactylus* [119], Ts19 Frag-II from *Tityus serrulatus* [120], OcyKTx2 from *Opisthacanthus cayaporum* [121], α-KTx 2.14 from *Rhopalurus garridoi* [122] and TstβKTx from *Tityus stigmurus* [123]. *Centruroides margaritatus* also expresses toxins selective against K_v1.1, K_v1.2, or K_v1.3, such as Cm28 and Cm39 [124,125]. Many of these scorpion toxins have drawn attention due to their pharmacological potential [126]. In agreement with earlier reports by a Mexican group describing the presence of regulators or the ERG K^+ channels, ergtoxins, in the *Centruroides* genus [127], a recent Mexico-Colombian collaboration reported a very potent (IC_{50} 3.4±0.2 nM in patch-clamp experiments), hERG1 inhibitor, the CmERG1 toxin, in the venom of *Centruroides margaritatus* [101]. The presence of this type of toxin could partially explain the cardiovascular toxicity of the venom of *C. margaritatus* in mammals [101,128]. Finally, it is worth to mention Discrepin, a toxin from *Tityus discrepans,* which blocks K_v4.3 in several experimental models [129–131].

Spiders: ω-agatoxins, from the venom of the spider *Agelenopsis aperta*, act as a pore blocker of Ca_v, but also as a gating inhibitor [132]. A peptide of 41 amino acids from the tarantula *H. gigas* blocks R-type Ca^{2+} currents [133]. DW13.3 toxin from *Filistata hibernalis* acts as a potent blocker of all Ca^{2+} channel currents, except for T-type currents [134]. Huwentoxin-X from *Ornithoctonus huwena* is a specific blocker of N-type Ca^{2+} currents in rat dorsal root ganglion neurons [135]. ω-grammotoxin-SIA, isolated from the venom of the tarantula *Grammostola spatulata*, is an N- and P-type Ca^{2+} currents blocker when the neurons are depolarized until +50 mV and behaves as a gating modifier with further depolarizations [136]. Effects on gating properties of channels carrying P-type currents seem to be shared by other toxins, such as Lsp-1 from *Lycosa sp* [137]. Some spider toxins also interact similarly with K^+ channels, as illustrated by the effect of HpTx2 from *Heteropoda venatoria* as a gating modifier on the K_v4 channels [138]. Interestingly, the venom of the Chinese tarantula *Chilobrachys jingzhao* has toxins (Jingzhaotoxins) with potent effects on Na_v, but which also affect K_v channels [139]. Phrixotoxins (PaTx1 and PaTx2) from the tarantula *Phrixotrichus auratus* specifically block K_v4.2 and K_v4.3, something that has helped understand the isoforms underlying some I_K currents in ventricular cardiomyocytes of mammalians [140].

Twelve species of *Pamphobeteus* and many of the famous *Phoneutria genus* (e.g., *P. depilata, P. reidyi, P. fera, and P. boliviensis)* have been characterized in South America [141,142]. Researchers from Colombia have described sequences similar to Theraphotoxin-Pn1a, Theraphotoxin-Pn1b, and Theraphotoxin-Pn2a, known to affect Ca_v, in the venom of *Pamphobeteus aff. nigricolor* [143]. Also using a bioinformatics approach, sequences with a high analogy to Ctenitoxins suggest that the venom of *Phoneutria boliviensis* may affect Ca_v2.1, 2.2, and 2.3 [144]. Recently, a rich source of new neurotoxin peptides that may act on Na_v and Ca_v channels was found in the venom gland of *Phoneutria depilata* by using transcriptomic and proteomic approaches [142]. Patch-clamp experiments become thus necessary since they will confirm or reject the conclusions regarding these *Pamphobeteus* and *Phoneutria* venoms. Promising results are expected for several reasons. For instance, previous studies by Brazilian researchers have already shown that the venoms of other species of the *Phoneutria* genus present in South America harbor Ca_v peptide blockers [145,146]. Also, other *Pamphobeteus* spiders, such as *P. verdolaga,* a recently described species from the Colombian Andes [147], showed potential antibacterial and channel-interacting peptides in the transcriptomic analysis of its venom gland [148,149]. Preliminary assays using fluorescence showed that some fractions of the venom of this spider could block some Ca_v [150], a result recently confirmed by our group using the patch-clamp technique and several isolated toxins [151]. Moreover, researchers have found that other South American members of the Theraposidae family, such as *Grammostola sp.*, have toxins that block Ca_v and K_v [50,136]. Besides these genera, the recent discovery of four *Medionops* species in a Colombian arachnological collection [152] reminds us that much work is ahead for the characterization of "old" and novel venoms potentially rich in channel-modulating toxins.

Snakes: Besides the presence of ICK peptides, venoms from snakes are enriched in different types of toxins with effects on ion channels, such as the 3FTxs, CRISPs, and BPTI-Kunitz-type peptides [62]. Stejnihagin toxin from *Trimeresurus stejnegeri*, an Asian snake, and calciseptine, from *Dendroaspis polylepis polylepis,* an African snake, block I_{CaL} [153,154]. The dendrotoxins I and toxin K, from the latter snake, block K_v1.1 [155]. Other dendrotoxins targeting K_v1.1, K_v1.2, or K_v1.6 channels have been purified from the *Dendroaspis* genus as well [46,62]. Similarly, BF9 from *Bungarus fasciatus* blocks K_v1.3 [156].

BaltCRP of the South American *Bothrops alternatus* inhibits K_v1.1, K_v1.3, and K_v2.1 with a low affinity over 1 μM, but does not block K_v1.2, K_v1.4, K_v1.5, or K_v10.1, as reported by a Brazilian-Belgium collaboration [48]. The venoms of a variety of species of the *Micrurus* genus from the southern region of Brazil reversibly inhibit K_v1.3 [157], however, specific toxins have not been brought to light yet. The snake toxins have been recognized as potential therapeutic tools [62]. For instance, the exendin-4 toxin from the lizard Gila monster (*Heloderma suspectum*), present in Mexico and the United States, antagonizes pancreatic I_K, thus modulating the release of insulin. The effect of this toxin is mediated by the intracellular increase in cyclic adenosine monophosphate, in turn, produced by the exendin-4 activation of the glucagon-like peptide one receptor-mediated activation of trimeric G proteins. The indirect regulation of nanomolar concentrations of exendin-4 on I_K and also on I_{CaL} has been found useful as a tool for the treatment of type II diabetes and its complications [158–160].

Table 1 and Figure 3 summarize the molecular weight as well as the inhibitory or activatory potency of Central and South American toxins. Most toxins (82%) have a molecular weight between 2.5 and 4.5 kDa. Almost all toxins (96.4%) were reported to block ionic currents, while only one toxin (PiVIIA) was found to activate I_{Ca} (note that this toxin was included in Table 1 but it was not represented in Figure 3). A refined analysis of the inhibitory power of the toxins that block I_{Ca} or I_K shows that in 40.63% of the cases, an IC_{50} between 0 and 10 nM (very potent) was measured, in 28.12% of the times the IC_{50} was over 10 and up to 100 nM (potent), the values were over 100 but lower or equal than 1,000 nM in 25.00% (moderate potency) of the cases and 6.25% of assays had an IC_{50} larger than 1,000 nM (low potency). A final observation is that there is an overrepresentation of scorpion toxins, most of which have been tested only against I_K. Overall, the toxins characterized with patch-clamp methods in Central and South American laboratories typically weigh less than 4.5 kDa and are very potent or potent to inhibit I_{Ca} or I_K.

Next, we will discuss the main experimental models used to evaluate the effect of toxins on voltage-gated ion channels using electrophysiological techniques.

Cell-free and single-cell-based models

General concepts

Cell-free models such as artificial bilayer lipid membranes (BLM) or single cell-based models are the most used to study the effect of toxins on ion channels. BLMs were originally developed using lipid or proteolipid extracts of neural tissue. They were soon modified to combine different types of lipids and adsorb molecules to simulate an excitable system. However, these models were mostly used to measure membrane biophysical properties (thickness, capacitance, resistance, and osmotic permeability) [161–163]. Later on, synthetic peptides or toxins inserted into phospholipids offered information on the possible features mediating the permeation pathway of ion channels [164,165]. Even when this technique is costly and time-consuming and the assembled membranes are unstable, it offers very precise information at a single-channel level and it is continuously being refined, in such a way that during the last three decades, BLM became very popular as a complementary method to study the effect of toxins or ligands on purified ion channels [166–169].

Single cells can be either derived from living animals (primary culture) or cultured cell lines. Cardiomyocytes (see section Cardiomyocytes and neurons), neurons (see section

Table 1. Summary of the toxins with effect on voltage-gated ion channels characterized by patch-clamp in Central and South America[a]

Species	Toxin	[d]I_x	[e]MW (KDa)	[b]IC_{50} (nM)				Reference
				Cnidarian and cone snails	Snakes	Scorpions	Spiders	
Bunodosoma caissarum	BcsTx1	[f]K_v1.2	4.15	0.03				[49]
Bunodosoma caissarum	BcsTx2	K_v1.6	3.91	7.76				[49]
Conus spurius	sr11a	K_v1.6	3.65	640.00				[94]
Conus princeps	PiVIIA	[g]I_{CaT}, I_{CaN}	3.09	[c]3,000.00				[95]
Bothrops alternatus	BaltCRP	K_v1.1	24.40		1,000.00			[48]
Heloderma suspectum	Exendin-4	K_v	4.19		10.00			[159]
Heloderma suspectum	Exendin-4	[h]I_{CaL}	4.19		0.10			[160]
Centruroides noxius	Noxiustoxin (II-11)	K_v	4.19			390.00		[116]
Centruroides noxius	Cobatoxin 1	K_v1.1	3.73			500.00		[51]
Pandinus imperator	Pi1	K_v1.3	3.84			9.70		[117]
Pandinus imperator	Pi2	K_v1.3	4.04			0.05		[117]
Pandinus imperator	Pi3	K_v1.3	4.07			0.50		[117]
Tityus cambridgei	Tc30	K_v1.3	3.87			15.90		[118]
Tityus cambridgei	Tc32	K_v1.3	3.52			9.90		[118]
Anuroctonus phaiodactylus	Anuroctoxin	K_v1.3	4.08			0.73		[119]
Tityus serrulatus	Ts19 Frag-II	K_v1.2	5.53			544.00		[120]
Opisthacanthus cayaporum	OcyKTx2	K_v1.3	3.81			18.00		[121]
Rhopalurus garridoi	α-KTx 2.14	K_v1.1	3.94			1,000.00		[122]
Tityus stigmurus	TstβKTx	K_v1.1	6.72			96.00		[123]
Centruroides margaritatus	Cm38	K_v1.2	2.82			0.96		[125]
Centruroides margaritatus	Cm38	K_v1.3	2.82			1.30		[125]
Centruroides margaritatus	Cm39	K_v1.2	3.98			65.00		[124]
Centruroides margaritatus	CmERG1	K_v11.1	4.79			3.40		[101]
Centruroides elegans elegans	CeERG4	K_v11.1	4.76			12.80		[127]
Tityus discrepans	Discrepin	K_v4.3	4.17			190.00		[129]
Phoneutria nigriventer	Tx3-2	I_{CaL}	3.55				280.00*	[145]
Grammostola spatulata	Grammotoxin	[i]I_{CaP}	4.10				50.00*	[136]
Grammostola iheringi	GiTx1	K_v4.3	3.58				2,000.00*	[50]
Grammostola iheringi	GiTx1	K_v11.1	3.58				3,695.00	[50]
Phrixotrichus auratus	PaTx1	K_v4.3	3.55				28.00	[140]
Phrixotrichus auratus	PaTx2	K_v4.3	3.92				71.00	[140]
Phrixotrichus auratus	PaTx1	K_v4.2	3.55				5.00	[140]
Phrixotrichus auratus	PaTx2	K_v4.2	3.92				34.00	[140]

[a]A total of 28 different toxins have 33 entries in the table since some toxins modulate both I_{Ca} and I_K or more than one channel isoform. Values were either directly taken (when experimentally measured) or estimated (based on extrapolations when not experimentally determined) from the results presented in the cited references. *From those estimated, these three values are considered most likely overestimated given the poor information available in the original papers. [b]IC_{50}, inhibitory concentration 50, applies for all toxins in the table, except for PiVIIA of *Conus princeps*; [c]This is the only effective concentration 50 (EC_{50}) value in the table, since this toxin activates $I_{Ca,}$ instead of inhibiting it; [d]I_x, ionic current; [e]MW, molecular weight; [f]K_v, K^+ channel isoform; [g]$I_{CaT,}$ I_{CaN}, T-type Ca^{2+} current, N-type Ca^{2+} current; [h]I_{CaL}, L-type Ca^{2+} current; [i]I_{CaP}, P-type Ca^{2+} current.

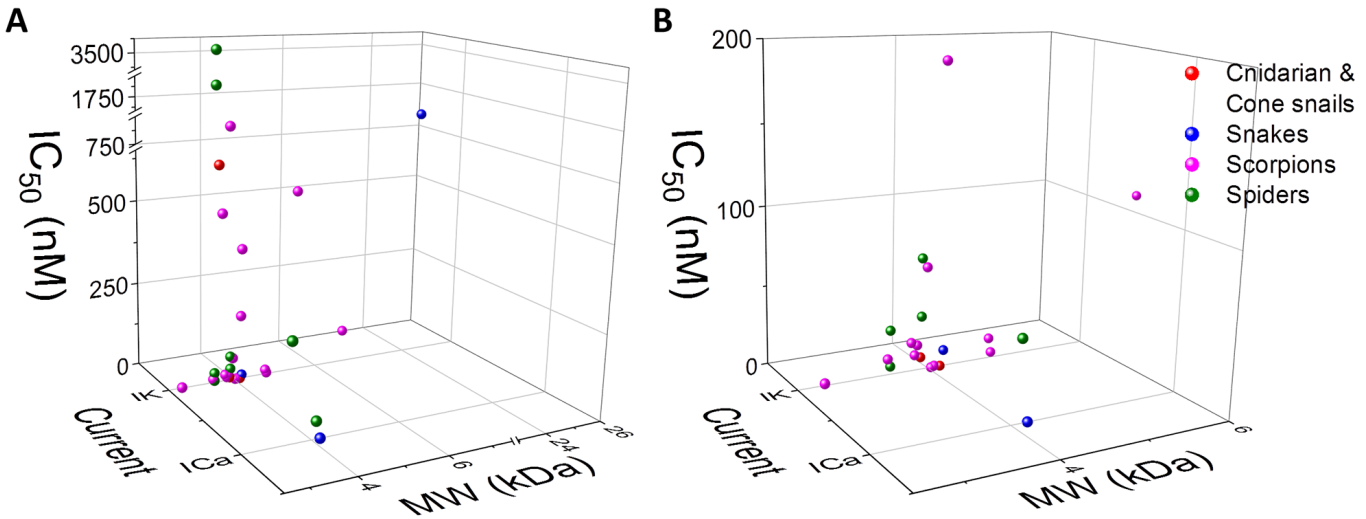

Figure 3. Dot plot of the molecular weight and inhibitory potency of the main toxins characterized by patch-clamp in Central and South America. **(A)** Toxins of cnidarian and cone snails (red dots), snakes (blue dots), scorpions (pink dots), and spiders (green dots) for which the molecular weight (MW) and inhibitory concentration 50 (IC_{50}) have been determined in Central and South American laboratories. **(B)** Zoom to the zone of high potency and low MW to better resolve the individual toxins. One toxin may have more than one entry if it has IC_{50} values determined for several channel isoforms or current types ($I_{Ca,}$ Ca^{2+} current; I_{K}, K^+ current). Additional file 1 shows the toxins labeled for their easier identification.

Cardiomyocytes and neurons), and T-lymphocytes are arguably the best mammalian primary culture models [119]. An alternative is using the non-mammalian oocytes from the frog *Xenopus laevis* [50,120,138,157]. When using cell lines, the best method is overexpressing the channels in the mammalian Human embryonic kidney (HEK) or Chinese hamster ovary (CHO) cells, or in the Sf9 insect cells [30,80,124,170].

Below, we will focus on cardiomyocytes and dorsal root ganglion neurons of mice as suitable primary cell models for the electrophysiological screening and evaluation of the effect of toxins on the ion channels of mammals. These two models offer advantages for many laboratories that may not be specialized in biophysical techniques: i) both are models of classical excitable cells in which a variety of macroscopic currents of sizeable amplitude can be obtained without excessive sources. Particularly, the presence of I_{Ca} makes them relevant to overcome the bias of the region in favor of evaluating the effects of toxins almost only on I_{K}, as demonstrated above, ii) the preclinical studies of promising molecules require cardiotoxicity studies, iii) they can be obtained from the same animal, thus reducing costs and fulfilling ethical requirements, iv) the information they give can be used to understand many effects of poisoning by multiple venomous species or for the treatment of some of the most prevalent diseases in mammals.

Cardiomyocytes

Cardiomyocytes are striated muscle cells that generate contractile force in the heart [171]. A spatially defined program of ion channels is required for the cardiomyocyte to regulate contractility through the excitation-contraction coupling phenomenon [172]. Although quite irregular, a typical adult murine cardiomyocyte is cylinder-like shaped, with a length of about 120-150 µm and a diameter of around 20-40 µm. In our laboratory, we typically found cardiomyocytes's capacitances between 105 and 160 pF (n=100). Cardiomyocytes have two separate nuclei, a highly organized array of myofilament proteins, and an extensive membranal T-tubule network with a high density of ion channels, particularly of Ca_v and K_v [173,174].

In ventricular cardiomyocytes, $Ca_v1.2$ is the most abundant isoform. It is the molecular entity responsible for the characteristic I_{CaL} found during phase two of the cardiac AP, which is activated at potentials more positive than -40 mV and reaches its peak amplitude between 0 and +10 mV [20,175]. The inactivation is biexponential, with a fast component described by a $\boldsymbol{\tau}_f$ between 12 and 16 ms and a slow component with $\boldsymbol{\tau}_s$ between 133 and 577 ms [174,176,177].

The presence of several K_v isoforms ($K_v1.1$, $K_v1.2$, $K_v1.4$, $K_v1.5$, $K_v1.7$, $K_v2.1$, $K_v3.1$, $K_v4.2$, $K_v4.3$, $K_v7.1$, $K_v11.1$) underlies the different K^+ currents measured in the heart (mainly the transient outward -I_{to}- and the delayed rectifiers -I_{Kur}, I_{Kr}, I_{Ks}-), and their differential distribution and degree of expression across the myocardium are responsible for the differences in shape and duration of the atrial and ventricular AP [20,23,32,178–181]. I_{to} is rapidly activated and contributes to phase one of the AP. Subtypes of I_{to} currents can be separated into fast ($K_v4.2$, $K_v4.3$) or slow ($K_v1.4$, $K_v1.7$) inactivation kinetics currents ($\boldsymbol{\tau}$ values between 25–80 ms for I_{tof} and 80–200 ms for I_{tos}) [23]. I_K ($K_v1.1$, $K_v1.2$, $K_v2.1$, $K_v1.5$, $K_v3.1$, $K_v7.1$, $K_v11.1$) contribute to the phases three and four of the AP and include the subtypes of currents: I_{Kur}, $I_{Kr,}$ and I_{Ks}. They typically activate at potentials more positive than -30 mV. I_{Kur} and I_{Kr} rapidly activate but become inactive with differential kinetics. On the contrary, I_{Ks} activate slowly but inactivate rapidly.

Dorsal root ganglion neurons

Spinal ganglia are located along the dorsal roots of the paraspinal nerves: cervical, thoracic, lumbar, and sacra. Inside these ganglia reside pseudo-unipolar neurons, which transport sensitive information from the skin and internal organs. These dorsal root ganglion (DRG) neurons are typically rounded, with a central nucleus, abundant Golgi, and endoplasmic reticulum [182,183]. The DRG neurons are protected by other small cells (satellite cells), usually adhered to the neuronal soma [184]. Molecular markers such as neurofilament 200 and β-III-tubulin are abundant in the DRG neurons but absent in the support cells [185–187]. For this reason, they are markers used to differentiate cell populations in the DRG.

DRG neuronal populations can be classified according to cell soma diameter o peripheral conduction velocity (CV) as small (< 20 µm), intermediate (21-40 µm), and large (> 40 µm). The small cells (fibers C) are devoid of myelin and have low CV (0.7-2.3 m/s). The intermediate cells (fibers A-δ) are moderately myelinated and thus conduct at somewhat faster velocities (3-15 m/s). The larger cells (fibers Aβ y Aα) are robustly myelinated and reach very fast conduction velocities (20-80 m/s) [184,188]. Obtained from mice or rats, this cellular model is suitable for the study of the effect of toxins on Ca_v [95,189], K_v [50,95,190], Na_v [50,191,192], and other transporters [193], in patch-clamp experiments. These cells have membrane capacitances between 44.3±14.4 pF (fibers C) and 70.0±27.6 pF (fibers Aβ and Aα) and a typical resting membrane potential of -60.0 mV [188]. These neurons differentially express P/Q, N, R, and T-type Ca^{2+} currents [12]. I_K is also diverse in these types of neurons, where K_v1, K_v3, and K_v4 are the mainly expressed subfamilies [194,195].

Methodological aspects

Cardiomyocytes and neurons

Isolation of cardiomyocytes

To obtain a single-cell suspension of cardiomyocytes, the heart needs to be digested. However, cardiac cells are firmly adhered to each other by the intercalated disks and the extracellular matrix. Moreover, cardiomyocytes are susceptible to hypoxia, physiological deterioration, mechanical perturbations, nutrient availability, pH, temperature changes, ionic fluctuations, and enzymatic digestion [196]. A common procedure that guarantees a good quality of cardiomyocytes is the Langendorff technique [197]. The main principle of this method is to perfuse the heart with enzyme-containing solutions in a retrograde manner. The retrograde flow shuts the leaflets of the aortic valve so that the perfusion solution cannot enter the left ventricle, being thus evacuated into the coronary arteries [198] (Figure 4).

The procedure starts with the removal of the heart from the thoracic cavity of the animal model in no more than 2 minutes (Figure 4A). Adult mice of the Swiss Webster or C57BL/6, of 20-26 g, render good results. It is better to leave as much of the ascending aorta as possible, including the lungs, to facilitate cannulation. All solutions must be filtered with 0.22 µm nitrocellulose filters. The tissue is rapidly immersed twice in cold, Ca^{2+}-free Tyrode solution (in mM: NaCl 135, KCl 5.4, $MgCl_2$ 1, Glucose 10, HEPES 10, NaH_2PO_4 0.33, pH 7.3) with enoxaparin (1 mg/mL) (Figure 4B).

The aorta is then cannulated under a stereoscope, the lungs are removed, and the heart is transferred to the Langendorff system (Figure 4C and 4D). At this stage, the heart is perfused at a flow rate of 4.5 mL/min with Ca^{2+}-free Tyrode's solution, bubbled with 95% O_2 and 5% CO_2, and supplemented with 1 mg/mL collagenase (type 2; Worthington, Lakewood, NJ) and 0.1 mg/mL protease (type XIV; Sigma, St. Louis, MO); always kept at 37°C for ~20 min, until the heart becomes pale and soft to the touch (Figure 4E). Only the ventricles are transferred to a Petri dish containing warm Ca^{2+}-free Tyrode's solution and triturated into small pieces with forceps (Figure 4F). After a gentle agitation, dozens of isolated, intact cardiomyocytes appear in the solution (Figure 4G). Finally, small amounts of Ca^{2+} are slowly restored to the solution.

Isolation of dorsal root ganglion neurons

After removing the cardiopulmonary apparatus and the viscera, two longitudinal cuts are made on either side of the vertebral column and one transversal cut below vertebrae L6. The *longissimus* muscles are removed, and the vertebral column can then be divided into cervical, thoracic, and lumbar sections and kept in cold Ca^{2+}-free Tyrode's solution. New cuts in the sagittal plane along the vertebral canal will help expose the spinal cord and the associated right and left DRG (Figure 5A, 5B, and 5C). This method renders ~35 DRG per mouse [187,192,199].

The DRG neurons are then incubated in 3 mg/mL collagenase type 2 in Ca^{2+}-free Tyrode's solution at 37.5°C for ~60 min. After washing out the enzyme, the DRG neurons are again incubated in 2.5 mg/mL Trypsin in Ca^{2+}-free Tyrode's solution at 37.5°C for ~12 min. The DRG neurons can then be dissociated. A gentle centrifugation at room temperature helps concentrate the neurons, whose nature can be verified as shown in Figures 5D through 5F.

I_{Ca} and I_K studies

A setup for patch-clamp studies is shown in Figure 6A. Cleaning the glass capillaries can be considered the most important preparation step for patch-clamp experiments [200]. This can be achieved by soaking them in ultra-pure water for two hours and then fully heat-drying them in an oven. Furthermore, we always apply positive pressure inside the capillaries using a homemade holder connected to a syringe (Figure 6B). Micropipettes must be fabricated immediately with the clean capillaries, using the common two-stage process: pulling a capillary and thus heat polishing the 3-5 µm pipette tip. Schott glass capillaries (outside diameter 1.65 mm, inside diameter 1.20 mm, Schott

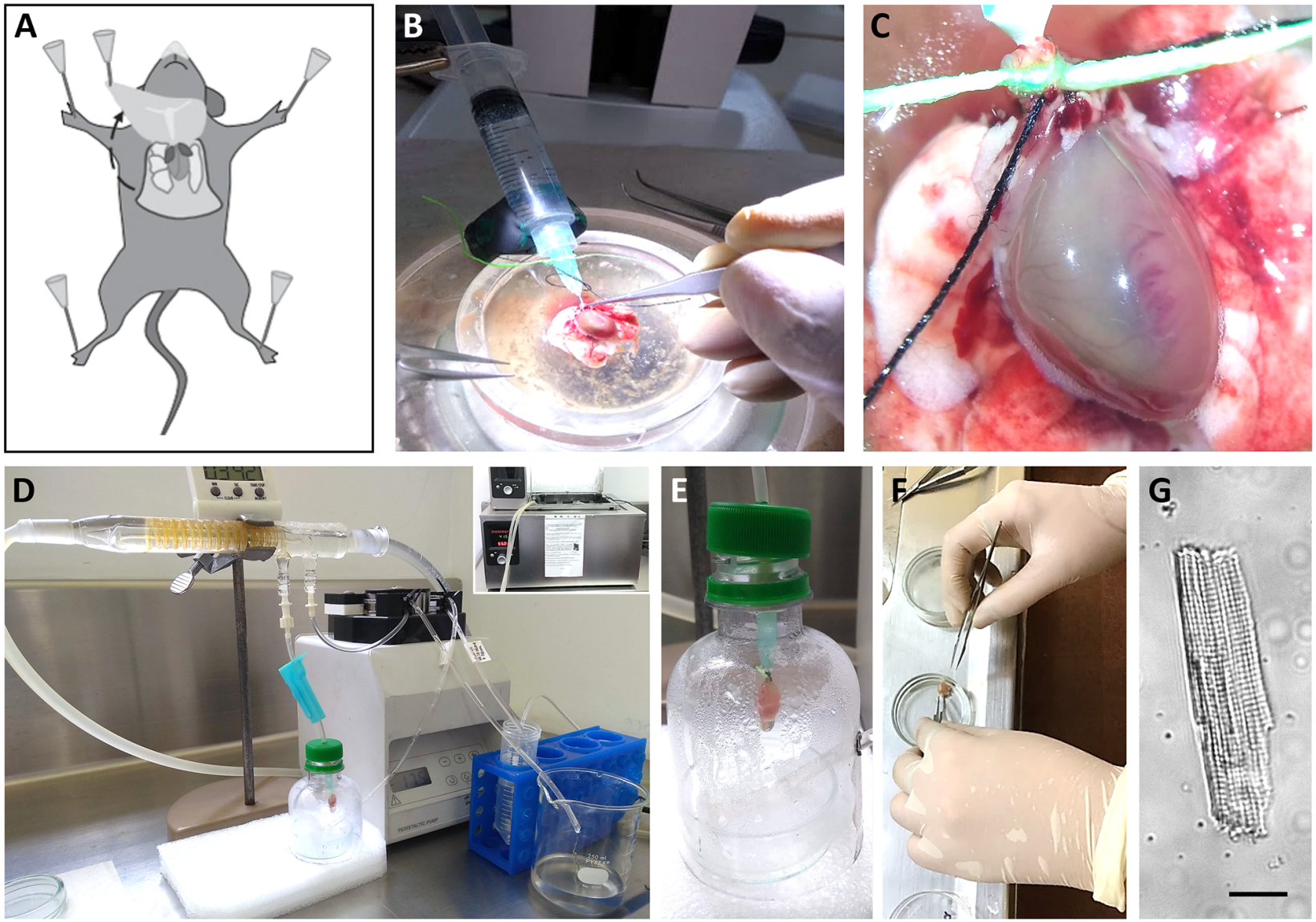

Figure 4. Schematic representation of murine cardiomyocytes isolation. **(A)** Procedure to pin the mouse´s limbs and gain access to the thoracic cavity. **(B, C)** Once the heart is removed, it should be rapidly mounted on the cannula, which is a shortened, tip-polished needle. Proper magnification allows the tying of the aorta to the cannula, with the help of two silk strands. Blood is then washed out by gently pushing the syringe-stored anticoagulant-supplemented Tyrode solution through the aorta. **(D)** The cannulated heart is transferred to the homemade Langendorff apparatus. It has a source of heated water (inset), a perfusion system driven by a pump, and a hoses network to ensure the solutions with different compositions reach the heart or are recycled. **(E)** A tight control of the temperature can be achieved by keeping the heart inside a closed chamber. **(F)** Once the heart has been enzymatically digested and looks pale, it is dismounted and minced with the help of forceps and scissors. **(G)** This procedure renders hundreds of isolated, living cardiomyocytes. Calibration bar: 50 µm.

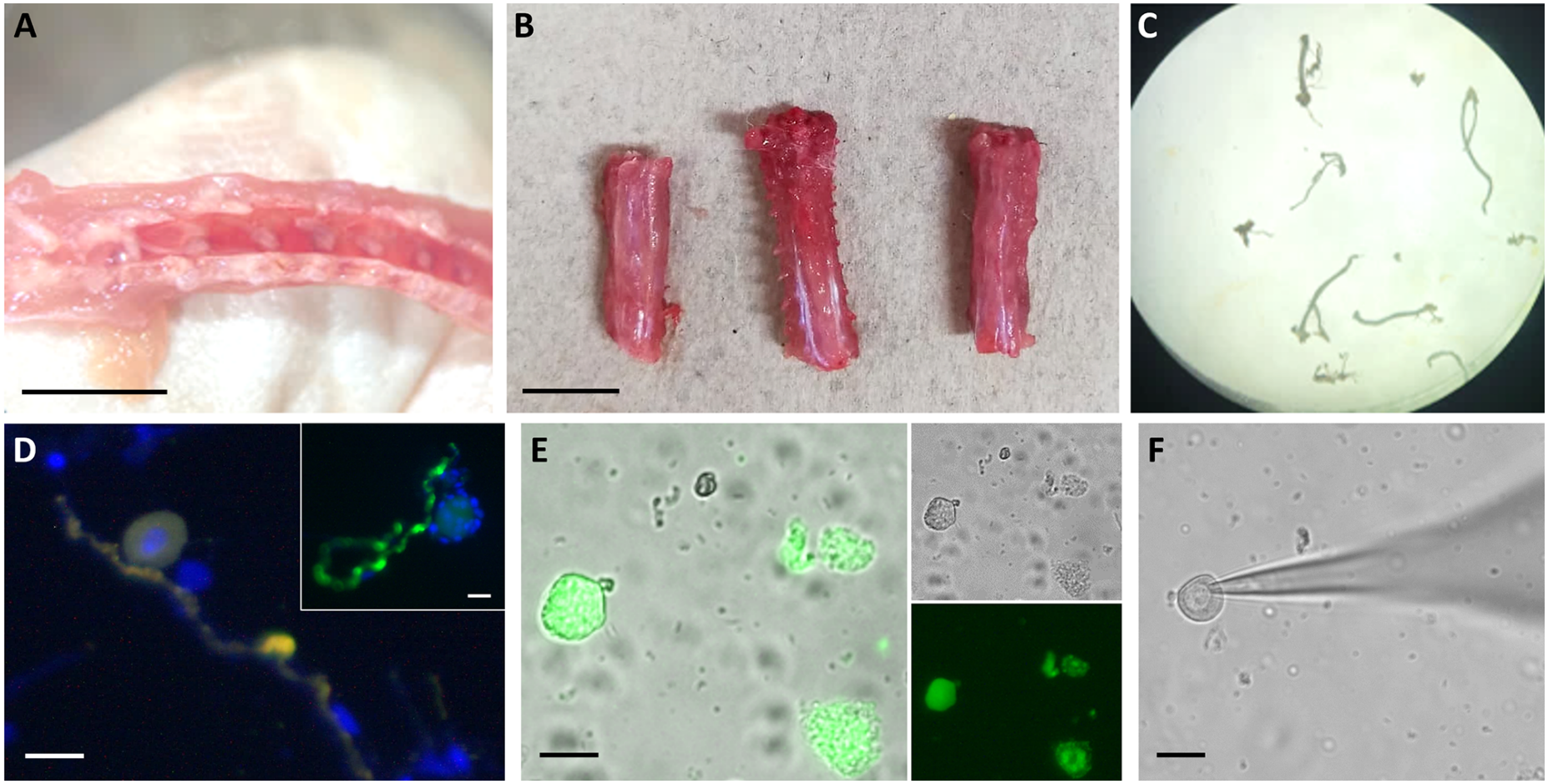

Figure 5. Schematic representation of murine dorsal root ganglion neuron isolation. **(A)** The ganglia look like dots inside the spine. **(B, C)** Dividing the spine into its cervical, thoracic, and lumbar parts makes ganglia removal easier. **(D)** After the enzymatic treatment, the identity of the isolated neurons can be characterized by demonstrating the positivity of the cells to neuron markers by fluorescence microscopy. In the large panel, the yellow color indicates the merge of the fluorescence channels imaging antibodies-labeled neurofilament 200 (originally labeled in green) and β-III-tubulin (originally labeled in red). The inset shows a different neuron only labeled for neurofilament 200 (green). Blue corresponds to nuclei, as labeled with Hoechst. Since each neuron has only one nucleus, other nuclei reflect the presence of small support cells still attached to some parts of the neurons. **(E)** The cells were loaded with the fluorescent Ca^{2+} dye Mag-Fluo-4. The large panel shows the merge of the bright field (upper inset) and the fluorescence field (lower inset). The appearance of the Ca^{2+} fluorescence (green) helps distinguish viable (leftmost cell) from non-viable (right, lowermost cell) cells because of the severe Ca^{2+} compartmentalization in the latter. **(F)** Demonstrates the feasibility of the path-clamp experiments in these neurons. The shadow coming from the right of the image corresponds to the patch clamp micropipette, which looks attached to the cell membrane at the leftmost part of the image. Calibration bars: 1 cm (A, B), 25 μm (D-F).

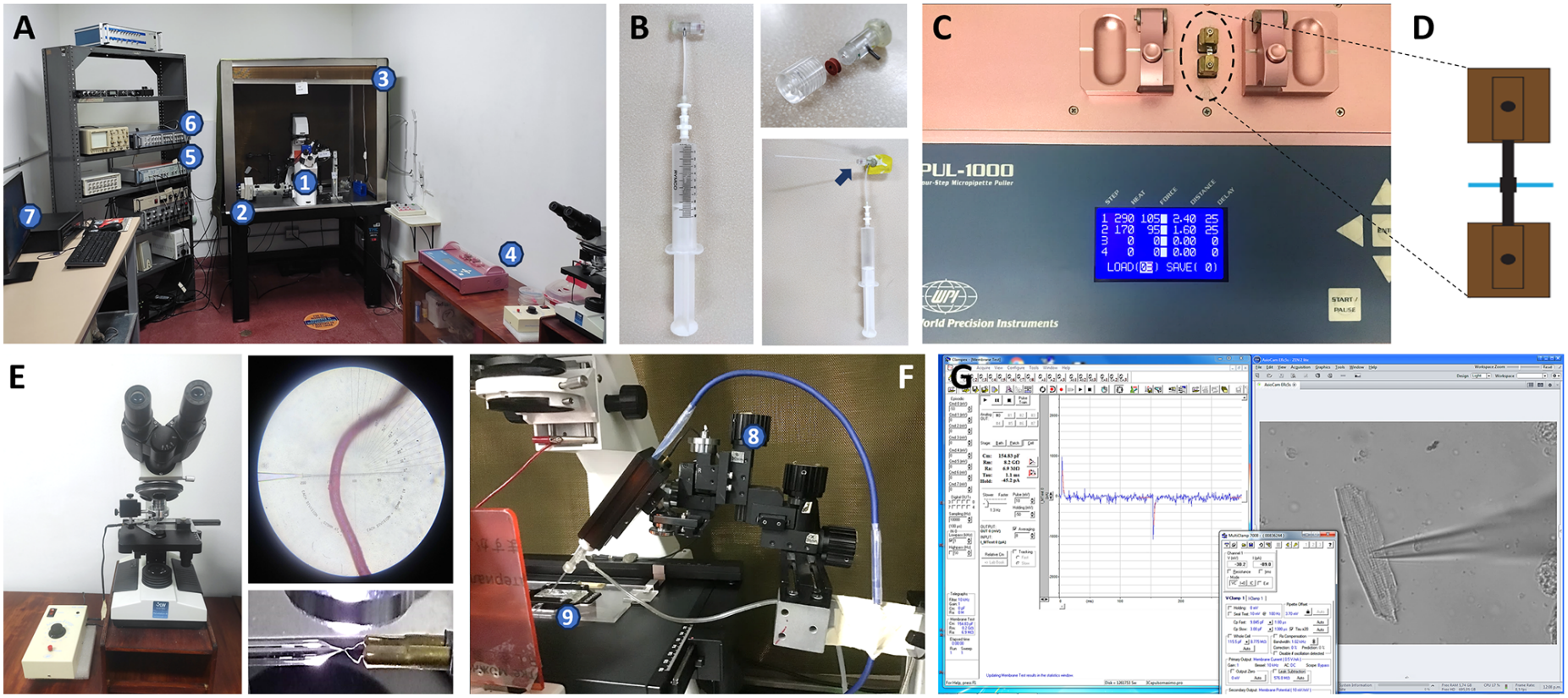

Figure 6. Electrophysiology setup for a patch-clamp experiment. **(A)** Electrophysiology setup. An inverted microscope (1) equipped with large magnification and a digital camera for adequate visualization of the working field (see panel **F** below) is mounted on an anti-vibration table (2) to reduce mechanical noise and is enclosed by a Faraday cage (3) to reduce electromagnetic noise. A nearby station to fabricate micropipettes includes a puller (4) and a microforge. On the left, the rack with the amplifier (5) and the digitizer (6), is close to the acquisition and processing hardware and software (7). **(B)** Home-made holder for cleaning the glass capillaries. This simple gadget is ensembled by tightly joining the embolus of a syringe to a hollow adapter (upper inset) through a thin silicone tube of 2-3 cm in length. Once the capillary is connected to the female port (blue arrow), air can be rapidly flushed to remove any dust from the inside of the capillary. **(C)** Typical protocol used to fabricate micropipettes by pulling the glass capillaries. The heating element, zoomed in **(D)**, heats the capillary (drawn in blue), allowing it to be stretched and split to form two micropipettes. **(E)** Each micropipette´s tip is forged with the help of a small, incandescent filament (red in the upper inset, as seen from the eyepiece of the microscope shown in **E**). A lateral view of the procedure is shown in the bottom inset (the micropipette coming from the left, and the filament from the right). **(F)** The forged micropipette is filled with the internal solution and mounted in the electrophysiology headstage equipped with an Ag/AgCl electrode, thus becoming a microelectrode. A micromanipulator (8) is then used to bring the recording microelectrode close to the isolated cells plated in the bath solution in the experimental chamber (9). A reference electrode put in the external solution closes the circuit. **(G)** Typical software configuration used in our laboratory. On the left, the interface of the recording software shows the conditions representative of a successful *whole-cell* experiment with a cardiomyocyte. After a gigaseal (> 1 GΩ) is formed, the cell membrane is ruptured, as effectively shown by the capacitive currents (peaks upwards and downwards) in the blue line and the numerical values of the parameters: *Cm* (membrane capacitance), *Rm* (membrane resistance), *Ra* (access resistance), *Tau* (time constant of decay of the capacitive peaks). On the right, the camera live image shows the seal between the microelectrode, coming from the right, and the cardiomyocyte. In the middle is the interface of the electrophysiology amplifier, in which the *voltage-clamp* mode is selected. After this moment, the ionic currents can be recorded.

8250 composition -today's equivalent of Corning's old 7052 glass-) give good results (Figure 6C, 6D and 6E).

Table 2 shows selected solutions used to perform patch-clamp experiments aimed at measuring I_{Ca} and I_K in different cellular models. While one solution type is inside the micropipette, the other solution type baths the cells. All solutions should be filtered through a cellulose filter.

Once the pipette is filled and mounted on the headstage of the patch-clamp setup, its tip is immersed into the bath solution, placed in the middle of the visual field, and checked. If the tip is clean and smooth and the pipette resistance is between 1.5 and 3 MΩ, it can be displaced until reaching close contact with the cellular membrane (Figure 6F and 6G). As long as the electrical values are satisfactory (seal is > 1 GΩ), the whole-cell configuration can be established by applying a small suction with a syringe. Complementarily, in devices equipped with a Zap circuit, a large (~ 1 V), brief (~ 0.1-10 ms) voltage pulse can be applied through the electrode, just by clicking on the Zap function of the interface program, thus increasing the probability of gaining access to the cytoplasm of the cell. Compensation of the Rs is usually adjusted up to 50% to minimize voltage control errors, and the P/4 protocol can be used to subtract leakage currents. The automatic fast and slow capacitance and whole-cell compensation functions are activated to reduce capacitances. Samples should be recorded at 10-20 kHz and can be low-pass filtered (Figure 6G).

The typical kinetics of I_{CaL} and I_K obtained in isolated cardiomyocytes are shown in Figure 7. The kinetics of the electrophysiological signals and their response to pharmacological modulators help experimentally confirm the identity and quality of the currents. For instance, under the stimulation protocols presented in Figure 7, and the appropriate solutions described in Table 2, I_{CaL} are inward currents, plotted as downward deflections (Figure 7A), with a maximum activation

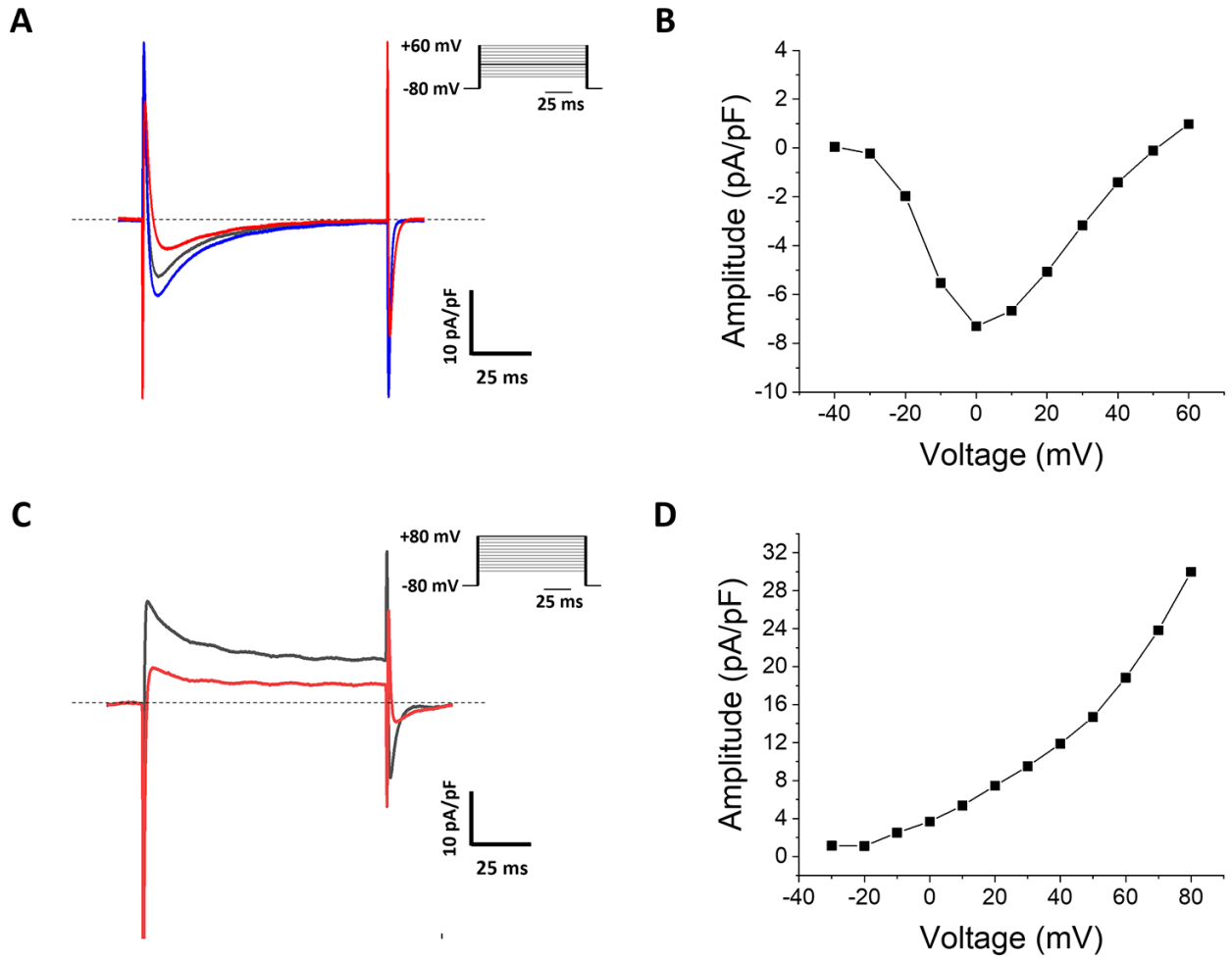

Figure 7. Typical currents and electrophysiological characterization of a peptide toxin from the *P. verdolaga* spider in isolated mouse cardiomyocytes. **(A)** I_{CaL} control (black), activated by 10 μM isoproterenol (blue) and blocked by 1 μM *vrdg177* (red), even in the presence of isoproterenol. Only the currents obtained at maximum activation are shown (voltage step highlighted in black in the voltage-clamp protocol). **(B)** An I_{CaL} current-voltage plot of a different cardiomyocyte obtained according to the steps of the voltage-clamp protocol shown in A. The maximum current activation is observed at 0 mV. **(C)** I_K control (black) and partially blocked by tetraethylammonium (red). Only the currents obtained at maximum activation are shown (voltage step highlighted in black in the voltage-clamp protocol). **(D)** An I_K current-voltage plot of a different cardiomyocyte obtained according to the steps of the voltage-clamp protocol shown in C. All analyzed currents had membrane seal resistances over 1 GΩ, with access resistances lower than 10 MΩ. Experiments were performed at room temperature.

Table 2. Selected solutions to perform patch-clamp experiments in different cellular models[a].

Cellular model, current [reference]	I_{Ca}						I_K							
	Cardiomyocytes, I_{CaL} [151,201]		HEK293T, I_{CaT} [47]		Dorsal root ganglion neurons, I_{Ca} [95]		Cardiomyocytes, I_K [151]		CHO, K_v11.1 [101]		Dorsal root ganglion neurons, I_K [95]		Peripheral blood mononuclear cells, K_v1.3 [125]	
	Pipette (mM)	Bath (mM)	Pipette (mM)	Bath (mM)	Pipette (mM)	Bath (mM)	Pipette (mM)	Bath (mM)	Pipette (mM)	Bath (mM)	Pipette (mM)	Bath (mM)	Pipette (mM)	Bath (mM)
NaCl			5	110				135	10	95				145
KCl							140	5.4		40	50	10		5
KF											40		140	
K^+ aspartate									130					
K^+ gluconate			140											
$CaCl_2$		1		10	0.1	2.5		1		2	0.1	1.8	1	2.5
$MgCl_2$		1	2	1			2	1	2	2		1.2	2	1
MgATP	5				2		4				2			
[b]HEPES	11	10	10	10	15	10	10	10	10	10	5	10	10	10
[b]EGTA	10		5		10		5		10		10		11	
D-glucose		10		10				10		5				5.5
[b]Chol-Cl											60	130		
CsCl	125	6		5	130	5								
CdCl								[c]0.3				0.3		
[b]TEA-Cl		140		30	10	130								
[b]TTX		0.1						0.1						
NaH_2PO_4								0.33						
Na_2GTP					1						1			
[b]4-AP						10								
pH	7.1 (adj. with CsOH)	7.4 (adj. with CsOH)	7.2 (adj. with KOH)	7.35 (adj. with TEA-OH)	7.2	7.4	7.2 (adj. with KOH)	7.2 (adj. with NaOH)	7.3 (adj. with NaOH)	7.3 (adj. with NaOH)	7.2	7.4	7.22	7.35
[d]Osmolarity (mOsm/L)	~280	~315	~295	~340	~310	~298	~308	~308	~308	~295	~320	~300	~310	~315

[a]Solutions used to measure I_{Ca} (Ca^{2+} currents) and I_K (K^+ currents) in different cellular models in different laboratories. [b]HEPES: 2-[4-(2-hydroxyethyl)piperazin-1-yl]ethanesulfonic acid; EGTA: 2-[2-[2-[2-[bis(carboxymethyl)amino]ethoxy]ethoxy]ethyl-(carboxymethyl)amino]acetic acid; Chol-Cl: Choline chloride; TEA-Cl: Tetraethylammonium chloride; TTX: tetrodotoxin; 4-AP: 4-Aminopyridine. [c]Nifedipine 10 µM can also be used. [d]These theoretical values overestimate by 5-10% of the expected real values because van´t Hoff corrections were not applied. HEK: human embryonic kidney cell line; CHO: Chinese hamster ovary cell line; I_{CaL}: L-type Ca^{2+} current; I_{CaT}: T-type Ca^{2+} current. K_v, K^+ channel isoform.

seen between 0 and +10 mV (Figure 7B) [175]. Classically, nifedipine (5-15 μM) blocks I_{CaL} while isoproterenol (1-10 μM) potentiates it (Figure 7A) [15,175,176]. In this preparation, the underlying molecular entity of I_{CaL} is $Ca_v1.2$ [20]. On the other hand, the protocol and solutions used for I_K in ventricular cardiomyocytes elicit macroscopic outward currents, graphed as upward deflections (Figure 7C), with maximum activation at +80 mV (Figure 7D). TEA (at high concentrations) and phrixotoxin-2 (100-300 nM) block this I_K [140]. This current mostly reflects the activation of $K_v4.2$, $K_v4.3$, $K_v1.4$, and $K_v1.7$ in this experimental model [20].

Study case

A new species of Tarantula was recently discovered in the Colombian Andes, named *Pamphobeteus verdolaga* [147]. This discovery represents a valuable opportunity to study novel toxins with potential use in physiology, pharmacology, and toxicology. A transcriptomic analysis of the venom gland of this species revealed polypeptide sequences which were confirmed to have antimicrobial properties [148,149]. Since some of the predicted toxins were short, bridged peptides, we hypothesized about a potential effect on ion channels. Several of these peptides were locally synthesized and screened for effects on ion channels. As a result, a few of them showed to be channel blockers [151]. Figure 7 shows currents (A and C) and current-voltage relationship plots (B and D) for I_{CaL} and I_K obtained in cardiomyocytes. *vrdg177* (*vrdg* stands for *verdolaga* and 177 comes from the transcriptomic analyses) at a concentration of 1 μM was able to block more than 50% of I_{CaL} in the illustrative recordings of Figure 7A. This peptide has 18 amino acids, a molecular weight of 2.3 kDa, a charge of +5, an isoelectric point of 9.8, water solubility higher than 4 mg/mL, and two disulfide bridges. As shown above (Figure 3), concentrations between 0.5 and 1 μM are within a good ballpark to start a screening of the potential effect of toxins on ion channels under electrophysiological approaches [202–205]. These results show that an initial screening identified spider toxins blocking I_{Ca}, as opposed to many other American toxins demonstrated to block I_K. This study case implies high novelty because spider venoms and toxins are barely studied with patch-clamp techniques and because it reflects a successful example of the comprehensive study of a toxin by implementing a multidisciplinary approach within one South American country. In this case, a national collaboration of several researchers allowed the description of the species and its taxonomic classification, then the local bioinformatic analyses of the peptide sequences permitted to demonstrate the potential of the new toxins, which led to the use of biochemical techniques to synthesize the peptides, whose success permitted the biophysical experiments which finally contributed to their electrophysiological characterization.

Conclusion

As this review did not search Chinese databases (e.g., Chinese Medical Current Content (CMCC), China National Knowledge Infrastructure (CNKI)), relevant information about toxins of Asian and African origin is likely underrepresented [206]. Also, toxins with an effect on voltage-gated Na^+ channels were excluded. This precluded us from deeply discussing very interesting and particular profiles of toxins such as OD-1. This toxin from the Iranian scorpion *Odonthobuthus doriae* specifically activates Na^+ currents, a property proven useful by a Taiwanese group to standardize a novel model of seizures and excitotoxicity [207], with multiple applications in biomedical research. However, the text highlights very interesting profiles of American toxins and keeps focused on the main aspects of its evaluation by patch-clamp, so the above limitations do not affect the main aims and conclusions of the review.

The main perspective implies that considerable effort should be made to better characterize the wealth of old and new molecules purified by many Latin American and Brazilian groups studying natural products. For instance, many venoms seem to have effects on ion channels, but specific channel-interacting toxins have not been isolated yet [92,157]. Marine sources are understudied in the region as channel modulators, even when the access to the sea is vast. Also, in earlier papers, the effects of many toxins were tested against a limited number of cellular models and channel isoforms, which hinders information about the selectivity of those toxins. The standardization of models for I_{Ca} studies is highly encouraged since a clear bias in favor of I_K analyses has thus arisen. This requires strengthening the electrophysiological capabilities in our region, which can be achieved by standardizing the use of the patch-clamp technique in different models. A network that brings together natural products research groups with biophysical research groups may also help to that aim. Our laboratory will be glad to be part of this network and collaborate with other laboratories in the region. This is relevant for the bioprospection of natural products in a continent rich in biodiversity and toxins that potently inhibit ion channels. Toxinological applications include the understanding of the venom complexity of a large number of species. Toxicology applications refer to the study of the mechanisms of action of toxins in potential prey and humans. Biotechnological applications comprise the exploration of potential applications of toxins as research, agricultural, or biomedical tools. Moreover, better collaborations can be done with research groups around the world.

In conclusion, the patch-clamp highlights as an electrophysiological technique relevant to the study of the potential effects of peptide toxins on voltage-gated ion channels. An initial evaluation can be implemented in cardiomyocytes and DRG neurons. Establishing these techniques in several laboratories across the region will strengthen the research capabilities in many fields, with copious potential applications.

Abbreviations

AP: action potential; BLM: bilayer lipid membranes; BPTI-Kunitz: bovine pancreatic trypsin inhibitor-Kunitz polypeptides; Ca_v: voltage-gated Ca^{2+} channels; CHO: Chinese hamster ovary; C_m: membrane capacitance; CRISP: cysteine-rich secretory proteins; CV: conduction velocity; DBP: disulfide bonding peptides; DDH: disulfide-directed β-hairpin; DHP: dihydropyridines; DPPX: dipeptidyl-aminopeptidase-like protein 6; DRG: dorsal root ganglion; EGTA: 2-[2-[2-[2-[bis(carboxymethyl)amino]ethoxy] ethoxy]ethyl-(carboxymethyl)amino]acetic acid; ERG: ether-a-go-go related gene; 3FTx: three-finger toxins; *g*: conductance; HEK: human embryonic kidney; HEPES: 2-[4-(2-hydroxyethyl) piperazin-1-yl]ethanesulfonic acid; I_C: capacitive current; I_{Ca}: Ca^{2+} current; ICK: inhibitor cystine knot motif; I_K: K^+ current; I_t: total current; I_x: ionic current; KchAP: K_v channel-associated protein; KChIP: K_v channel-interacting protein; KCNE: K^+ voltage-gated channel subfamily E regulatory subunit; KCNQ or KvLQT: K^+ voltage-gated channel subfamily Q member or voltage-gated K^+ channel isoform associated to long QT syndrome; K_v: voltage-gated K^+ channels; PD: pore domain; Rs: series resistance; SF: selectivity filter; SNR: signal-to-noise ratio; TEA: tetraethylammonium; TTX: tetrodotoxin; V_m: membrane potential; VSD: voltage sensing domain.

Acknowledgments

We thank Andrés Milán, Lorena Muñoz, Daniela Lopera and Norman Balcázar (University of Antioquia), and Pura Bolaños (Venezuelan Institute of Scientific Research) for technical support.

Availability of data and materials

Not applicable.

Funding

This research was funded by the Colombian Ministry of Science and Technology (MinCiencias, Grant 111577757673, to JCC, MAG and CS), grants E01792-B and ES03180101 (to JCC and MAG) from the Planning Office of the University of Antioquia, Colombia and the Instructor scholarship (2019-2020 to JR-P) from University of Antioquia, Colombia. Funders did not participate in selecting sources of evidence, analyses, manuscript writing, or submission.

Competing interests

The authors declare that they have no competing interests.

Authors' contributions

JR-P, AG-R, MAG, and JCC participated in the conception of the review, writing and preparing of the figures. JR-P and AG-R performed the patch-clamp experiments presented in the study case. CS-R and CS provided the toxin and gave intellectual input to the manuscript. All authors read and approved the final manuscript.

Ethics approval

Not applicable

Consent for publication

Not applicable.

Supplementary material

The following online material is available for this article:

Additional file 1. Dot plot of the molecular weight and inhibitory potency of the main toxins characterized by patch-clamp in Central and South America. All toxins were labelled with their names for their easier identification.

References

1. Hamill OP, Marty A, Neher E, Sakmann B, Sigworth FJ. Improved patch-clamp techniques for high-resolution current recording from cells and cell-free membrane patches. Pflugers Arch. 1981 Aug;391(2):85-100. doi: 10.1007/BF00656997.
2. Neher E, Sakmann B. Single-channel currents recorded from membrane of denervated frog muscle fibers. Nature. 1976 Apr 29;260(5554):799-802. doi: 10.1038/260799a0.
3. Sakmann B, Neher E. Patch clamp techniques for studying ionic channels in excitable membranes. Annu Rev Physiol. 1984;46:455-72. doi: 10.1146/annurev.ph.46.030184.002323.
4. Tricco AC, Lillie E, Zarin W, O'Brien KK, Colquhoun H, Levac D, Moher D, Peters MDJ, Horsley T, Weeks L, et al. PRISMA extension for scoping reviews (PRISMA-ScR): checklist and explanation. Ann Intern Med. 2018 Oct 2;169(7):467-473. doi: 10.7326/M18–0850.
5. Catterall WA. Structure and function of voltage-gated ion channels. Annu Rev Biochem. 1995;64:493-531. doi: 10.1146/annurev.bi.64.070195.002425.
6. Hodgkin AL, Huxley AF. A quantitative description of membrane current and its application to conduction and excitation in nerve. J Physiol. 1952 Aug;117(4):500-44. doi: 10.1113/jphysiol.1952.sp004764.
7. Quintana E, Torres Y, Alvarez C, Rojas A, Forero ME, Camacho M. Changes in macrophage membrane properties during early Leishmania amazonensis infection differ from those observed during established infection and are partially explained by phagocytosis. Exp Parasitol. 2010 Mar;124(3):258-64. doi: 10.1016/j.exppara.2009.10.006.
8. Bolaños P, Calderón JC. Excitation-contraction coupling in mammalian skeletal muscle: blending old and last-decade research. Front Physiol. 2022 Sep 2;13:989796. doi: 10.3389/fphys.2022.989796.
9. Catterall WA. Voltage-gated calcium channels. Cold Spring Harb Perspect Biol. 2011 Aug 1;3(8):a003947. doi: 10.1101/cshperspect.a003947.
10. Wu J, Yan Z, Li Z, Qian X, Lu S, Dong M, Zhou Q, Yan N. Structure of the voltage-gated calcium channel Ca(v)1.1 at 3.6 Å resolution. Nature. 2016 Sep 8;537(7619):191-196. doi: 10.1038/nature19321.
11. Zhao Y, Huang G, Wu J, Wu Q, Gao S, Yan Z, Lei J, Yan N. Molecular basis for ligand modulation of a mammalian voltage-gated Ca2+ channel. Cell. 2019 May 30;177(6):1495-1506.e12. doi: 10.1016/j.cell.2019.04.043.
12. Kushnir A, Marx SO. Voltage-gated calcium channels. In: Zipes DP, Jalife J, Stevenson WG, editors. Card Electrophysiol From Cell to Bedside. 7th ed. Elsevier; 2018. p. 12–24.
13. Catterall WA. Ion channel voltage sensors: structure, function, and pathophysiology. Neuron. 2010 Sep 23;67(6):915-28. doi: 10.1016/j.neuron.2010.08.021.
14. Pangrsic T, Singer JH, Koschak A. Voltage-gated calcium channels: key players in sensory coding in the retina and the inner ear. Physiol Rev. 2018 Oct 1;98(4):2063-2096. doi: 10.1152/physrev.00030.2017.
15. Alexander SP, Mathie A, Peters JA, Veale EL, Striessnig J, Kelly E, Armstrong JF, Faccenda E, Harding SD, Pawson AJ, et al. The concise guide to pharmacology 2021/22: ion channels. Br J Pharmacol. 2021 Oct;178 Suppl 1:S157-S245. doi: 10.1111/bph.15539.

16. Mesirca P, Torrente AG, Mangoni ME. Functional role of voltage gated Ca(2+) channels in heart automaticity. Front Physiol. 2015 Feb 2;6:19. doi: 10.3389/fphys.2015.00019.
17. Vink S, Alewood PF. Targeting voltage-gated calcium channels: developments in peptide and small-molecule inhibitors for the treatment of neuropathic pain. Br J Pharmacol. 2012 Nov;167(5):970-89. doi: 10.1111/j.1476–5381.2012.02082.x.
18. Mouhat S, Andreotti N, Jouirou B, Sabatier JM. Animal toxins acting on voltage-gated potassium channels. Curr Pharm Des. 2008;14(24):2503-18. doi: 10.2174/138161208785777441.
19. Ranjan R, Logette E, Marani M, Herzog M, Tâche V, Scantamburlo E, Buchillier V, Markram H. A kinetic map of the homomeric voltage-gated potassium channel (Kv) family. Front Cell Neurosci. 2019 Aug 20;13:358. doi: 10.3389/fncel.2019.00358.20.
20. Grunnet M. Repolarization of the cardiac action potential. Does an increase in repolarization capacity constitute a new anti-arrhythmic principle? Acta Physiol (Oxf). 2010 Feb;198 Suppl 676:1-48. doi: 10.1111/j.1748–1716.2009.02072.x.
21. Armstrong CM. Voltage-gated K channels. Sci STKE. 2003 Jun 24;2003(188):re10. doi: 10.1126/stke.2003.188.re10.
22. Wulff H, Castle NA, Pardo LA. Voltage-gated potassium channels as therapeutic targets. Nat Rev Drug Discov. 2009 Dec;8(12):982-1001. doi: 10.1038/nrd2983.
23. Oudit GY, Backx PH. Voltage-Gated Potassium Channels. In: Zipes DP, Jalife J, Stevenson WG, editors. Card Electrophysiol From Cell to Bedside. 7th ed. Elsevier; 2018. p. 25–37.
24. Jiang Y, Lee A, Chen J, Cadene M, Chait BT, MacKinnon R. The open pore conformation of potassium channels. Nature. 2002 May 30;417(6888):523-6. doi: 10.1038/417523a.
25. Doyle DA, Cabral JM, Pfuetzner RA, Kuo A, Gulbis JM, Cohen SL, Chait BT, MacKinnon R. The structure of the potassium channel: molecular basis of K+ conduction and selectivity. Science. 1998 Apr 3;280(5360):69-77. doi: 10.1126/science.280.5360.69.
26. Bernèche S, Roux B. Energetics of ion conduction through the K+ channel. Nature. 2001 Nov 1;414(6859):73-7. doi: 10.1038/35102067.
27. Kuryshev YA, Gudz TI, Brown AM, Wible BA. KChAP as a chaperone for specific K(+) channels. Am J Physiol Cell Physiol. 2000 May;278(5):C931-41. doi: 10.1152/ajpcell.2000.278.5.C931.
28. Pongs O, Leicher T, Berger M, Roeper J, Bähring R, Wray D, Giese KP, Silva AJ, Storm JF. Functional and molecular aspects of voltage-gated K+ channel beta subunits. Ann N Y Acad Sci. 1999 Apr 30;868:344-55. doi: 10.1111/j.1749–6632.1999.tb11296.x.
29. Morin TJ, Kobertz WR. A derivatized scorpion toxin reveals the functional output of heteromeric KCNQ1-KCNE K+ channel complexes. ACS Chem Biol. 2007 Jul 20;2(7):469-73. doi: 10.1021/cb700089s.
30. Roeper J, Sewing S, Zhang Y, Sommer T, Wanner SG, Pongs O. NIP domain prevents N-type inactivation in voltage-gated potassium channels. Nature. 1998 Jan 22;391(6665):390-3. doi: 10.1038/34916.
31. Oliveras A, Roura-Ferrer M, Solé L, de la Cruz A, Prieto A, Etxebarria A, Manils J, Morales-Cano D, Condom E, Soler C, et al. Functional assembly of Kv7.1/Kv7.5 channels with emerging properties on vascular muscle physiology. Arterioscler Thromb Vasc Biol. 2014 Jul;34(7):1522-30. doi: 10.1161/ATVBAHA.114.303801.
32. Guo W, Li H, Aimond F, Johns DC, Rhodes KJ, Trimmer JS, Nerbonne JM. Role of heteromultimers in the generation of myocardial transient outward K+ currents. Circ Res. 2002 Mar 22;90(5):586-93. doi: 10.1161/01.res.0000012664.05949.e0.
33. Yellen G. The voltage-gated potassium channels and their relatives. Nature. 2002 Sep 5;419(6902):35-42. doi: 10.1038/nature00978.
34. Piedras-Rentería ES, Barrett CF, Cao YQ, Tsien RW. Voltage-gated calcium channels, calcium signaling, and channelopathies. New Compr Biochem. 2007;41:127–66. doi: 10.1016/S0167–7306(06)41005–X
35. The Nobel Prize. The Nobel Prize in Physiology or Medicine 1991 [Internet]. 1991 [cited 2023 Jul 17]. Available from: https://www.nobelprize.org/prizes/medicine/1991/summary/
36. Conforti L. Patch-Clamp Techniques. In: Sperelakis N, editor. Cell Physiol Sourcebook. 4th ed. Elsevier; 2012. p. 369–81.
37. Kornreich BG. The patch clamp technique: principles and technical considerations. J Vet Cardiol. 2007 May;9(1):25-37. doi: 10.1016/j.jvc.2007.02.001.
38. Kodirov SA. Whole-cell patch-clamp recording and parameters. Biophys Rev. 2023 Apr 10;15(2):257-288. doi: 10.1007/s12551–023–01055–8.
39. Petkov G V. Ion channels. In: Miles H, Messer WS, Bachmann KA, editors. Pharmacol Princ Pract. Academic Press; 2009. p. 387–427.
40. Perkins KL. Cell-attached voltage-clamp and current-clamp recording and stimulation techniques in brain slices. J Neurosci Methods. 2006 Jun 30;154(1-2):1-18. doi: 10.1016/j.jneumeth.2006.02.010.
41. Boron WF, Boulpaep EL. Medical Physiology: A Cellular and Molecular Approach. 2nd ed. Philadelphia: Elsevier Saunders; 2012.
42. Polder HR, Weskamp M, Linz K, Meyer R. Voltage-clamp and patch-clamp techniques. In: Dhein S, Mohr FW, Delmar, editors. Practical Methods in Cardiovascular Research. Springer Nature:2005;272–323.
43. Levis RA, Rae JL. Low-noise patch-clamp techniques. Methods Enzymol. 1998;293:218-66. doi: 10.1016/s0076–6879(98)93017–8.
44. Colquhoun D, Sigworth FJ. Fitting and Statistical Analysis of Single-Channel Records. In: Sakmann B, Neher E, editors. Single-Channel Recording. New York: Plenum Press; 1983. p. 191–263.
45. Sherman AJ, Shrier A, Cooper E. Series resistance compensation for whole-cell patch-clamp studies using a membrane state estimator. Biophys J. 1999 Nov;77(5):2590-601. doi: 10.1016/S0006–3495(99)77093–1.
46. Imredy JP, Chen C, MacKinnon R. A snake toxin inhibitor of inward rectifier potassium channel ROMK1. Biochemistry. 1998 Oct 20;37(42):14867-74. doi: 10.1021/bi980929k.
47. Hackney CM, Flórez Salcedo P, Mueller E, Koch TL, Kjelgaard LD, Watkins M, Zachariassen LG, Tuelung PS, McArthur JR, Adams DJ, et al. A previously unrecognized superfamily of macro-conotoxins includes an inhibitor of the sensory neuron calcium channel Cav2.3. PLoS Biol. 2023 Aug 3;21(8):e3002217. doi: 10.1371/journal.pbio.3002217.
48. Bernardes CP, Menaldo DL, Zoccal KF, Boldrini-França J, Peigneur S, Arantes EC, Rosa JC, Faccioli LH, Tytgat J, Sampaio SV. First report on BaltCRP, a cysteine-rich secretory protein (CRISP) from Bothrops alternatus venom: Effects on potassium channels and inflammatory processes. Int J Biol Macromol. 2019 Nov 1;140:556-567. doi: 10.1016/j.ijbiomac.2019.08.108.
49. Orts DJ, Peigneur S, Madio B, Cassoli JS, Montandon GG, Pimenta AM, Bicudo JE, Freitas JC, Zaharenko AJ, Tytgat J. Biochemical and electrophysiological characterization of two sea anemone type 1 potassium toxins from a geographically distant population of Bunodosoma caissarum. Mar Drugs. 2013 Mar 6;11(3):655-79. doi: 10.3390/md11030655.
50. Montandon GG, Cassoli JS, Peigneur S, Verano-Braga T, Santos DMD, Paiva ALB, Moraes ÉR, Kushmerick C, Borges MH, Richardson M, et al. GiTx1(β/κ-theraphotoxin-Gi1a), a novel toxin from the venom of Brazilian tarantula Grammostola iheringi (Mygalomorphae, Theraphosidae): Isolation, structural assessments and activity on voltage-gated ion channels. Biochimie. 2020 Sep;176:138-149. doi: 10.1016/j.biochi.2020.07.008.
51. Selisko B, Garcia C, Becerril B, Gómez-Lagunas F, Garay C, Possani LD. Cobatoxins 1 and 2 from Centruroides noxius Hoffmann constitute a subfamily of potassium-channel-blocking scorpion toxins. Eur J Biochem. 1998 Jun 15;254(3):468-79. doi: 10.1046/j.1432–1327.1998.2540468.x.
52. Casewell NR, Wüster W, Vonk FJ, Harrison RA, Fry BG. Complex cocktails: the evolutionary novelty of venoms. Trends Ecol Evol. 2013 Apr;28(4):219-29. doi: 10.1016/j.tree.2012.10.020.
53. Rash LD, Hodgson WC. Pharmacology and biochemistry of spider venoms. Toxicon. 2002 Mar;40(3):225-54. doi: 10.1016/s0041–0101(01)00199–4.
54. Bolon B, Heinz-Taheny K, Yeung K, Oguni J, Erickson T, Chai PR, Goldfine. Animal toxins. In: Heinz-taheny K, Rudmann D, Mahler B, editors. Haschek and Rousseaux's Handbook of Toxicologic Pathology. 4th ed. Academic Press; 2023. p. 547–628.
55. Xia Z, He D, Wu Y, Kwok HF, Cao Z. Scorpion venom peptides: Molecular diversity, structural characteristics, and therapeutic use from channelopathies to viral infections and cancers. Pharmacol Res. 2023 Nov;197:106978. doi: 10.1016/j.phrs.2023.106978.

56. Jin AH, Muttenthaler M, Dutertre S, Himaya SWA, Kaas Q, Craik DJ, Lewis RJ, Alewood PF. Conotoxins: Chemistry and Biology. Chem Rev. 2019 Nov 13;119(21):11510-11549. doi: 10.1021/acs.chemrev.9b00207.
57. Quintero-Hernández V, Jiménez-Vargas JM, Gurrola GB, Valdivia HH, Possani LD. Scorpion venom components that affect ion-channels function. Toxicon. 2013 Dec 15;76:328-42. doi: 10.1016/j.toxicon.2013.07.012.
58. King GF, Hardy MC. Spider-venom peptides: structure, pharmacology, and potential for control of insect pests. Annu Rev Entomol. 2013;58:475-96. doi: 10.1146/annurev–ento–120811–153650.
59. King G. Venoms to drugs: translating venom peptides into therapeutics. Aust Biochem. 2013 Dec 3;44:13–6.
60. Daly NL, Craik DJ. Bioactive cystine knot proteins. Curr Opin Chem Biol. 2011 Jun;15(3):362-8. doi: 10.1016/j.cbpa.2011.02.008.
61. Langenegger N, Nentwig W, Kuhn-Nentwig L. Spider venom: components, modes of action, and novel strategies in transcriptomic and proteomic analyses. Toxins (Basel). 2019 Oct 22;11(10):611. doi: 10.3390/toxins11100611.
62. AlShammari AK, Abd El-Aziz TM, Al-Sabi A. Snake venom: a promising source of neurotoxins targeting voltage-gated potassium channels. Toxins (Basel). 2023 Dec 25;16(1):12. doi: 10.3390/toxins16010012.
63. Ojeda PG, Ramírez D, Alzate-Morales J, Caballero J, Kaas Q, González W. Computational studies of snake venom toxins. Toxins (Basel). 2017 Dec 22;10(1):8. doi: 10.3390/toxins10010008.
64. Reeks TA, Fry BG, Alewood PF. Privileged frameworks from snake venom. Cell Mol Life Sci. 2015 May;72(10):1939-58. doi: 10.1007/s00018–015–1844–z.
65. Tadokoro T, Modahl CM, Maenaka K, Aoki-Shioi N. Cysteine-rich secretory proteins (CRISPs) from venomous snakes: an overview of the functional diversity in a large and underappreciated superfamily. Toxins (Basel). 2020 Mar 12;12(3):175. doi: 10.3390/toxins12030175.
66. Deplazes E. Molecular Simulations of Disulfide-Rich Venom Peptides with Ion Channels and Membranes. Molecules. 2017 Feb 27;22(3):362. doi: 10.3390/molecules22030362.
67. Dutertre S, Lewis RJ. Use of venom peptides to probe ion channel structure and function. J Biol Chem. 2010 Apr 30;285(18):13315-20. doi: 10.1074/jbc.R109.076596.
68. MacKinnon R. Determination of the subunit stoichiometry of a voltage-activated potassium channel. Nature. 1991 Mar 21;350(6315):232-5. doi: 10.1038/350232a0.
69. Chen J, Liu X, Yu S, Liu J, Chen R, Zhang Y, Jiang L, Dai Q. A novel ω-conotoxin Bu8 inhibiting N-type voltage-gated calcium channels displays potent analgesic activity. Acta Pharm Sin B. 2021 Sep;11(9):2685-2693. doi: 10.1016/j.apsb.2021.03.001.
70. Gao Y, Bai L, Zhou W, Yang Y, Zhang J, Li L, Jiang M, Mi Y, Li TT, Zhang X, Zhang W, Xu JT. PARP-1-regulated TNF-α expression in the dorsal root ganglia and spinal dorsal horn contributes to the pathogenesis of neuropathic pain in rats. Brain Behav Immun. 2020 Aug;88:482-496. doi: 10.1016/j.bbi.2020.04.019.
71. Liu Z, Deng M, Xiang J, Ma H, Hu W, Zhao Y, Li DW, Liang S. A novel spider peptide toxin suppresses tumor growth through dual signaling pathways. Curr Mol Med. 2012 Dec;12(10):1350-60. doi: 10.2174/156652412803833643.
72. Wang Y, Wang L, Yang H, Xiao H, Farooq A, Liu Z, Hu M, Shi X. The Spider Venom Peptide Lycosin-II Has Potent Antimicrobial Activity against Clinically Isolated Bacteria. Toxins (Basel). 2016 Apr 26;8(5):119. doi: 10.3390/toxins8050119.
73. Xie W, Strong JA, Zhang JM. Local knockdown of the NaV1.6 sodium channel reduces pain behaviors, sensory neuron excitability, and sympathetic sprouting in rat models of neuropathic pain. Neuroscience. 2015 Apr 16;291:317-30. doi: 10.1016/j.neuroscience.2015.02.010.
74. Hodgson WC, Isbister GK. The application of toxins and venoms to cardiovascular drug discovery. Curr Opin Pharmacol. 2009 Apr;9(2):173-6. doi: 10.1016/j.coph.2008.11.007.
75. Pennington MW, Czerwinski A, Norton RS. Peptide therapeutics from venom: Current status and potential. Bioorg Med Chem. 2018 Jun 1;26(10):2738-2758. doi: 10.1016/j.bmc.2017.09.029.
76. Robinson SD, Vetter I. Pharmacology and therapeutic potential of venom peptides. Biochem Pharmacol. 2020 Nov;181:114207. doi: 10.1016/j.bcp.2020.114207.
77. Fiorotti HB, Figueiredo SG, Campos FV, Pimenta DC. Cone snail species off the Brazilian coast and their venoms: a review and update. J Venom Anim Toxins incl Trop Dis. 2023 Jan 27;29:e20220052. doi: 10.1590/1678–9199–JVATITD–2022–0052.
78. Frazão B, Vasconcelos V, Antunes A. Sea anemone (Cnidaria, Anthozoa, Actiniaria) toxins: an overview. Mar Drugs. 2012 Aug;10(8):1812-1851. doi: 10.3390/md10081812.
79. Smallwood TB, Clark RJ. Advances in venom peptide drug discovery: where are we at and where are we heading? Expert Opin Drug Discov. 2021 Oct;16(10):1163-1173. doi: 10.1080/17460441.2021.1922386.
80. Selvakumar P, Fernández-Mariño AI, Khanra N, He C, Paquette AJ, Wang B, Huang R, Smider VV, Rice WJ, Swartz KJ, Meyerson JR. Structures of the T cell potassium channel Kv1.3 with immunoglobulin modulators. Nat Commun. 2022 Jul 4;13(1):3854. doi: 10.1038/s41467–022–31285–5.
81. Bourinet E, Zamponi GW. Block of voltage-gated calcium channels by peptide toxins. Neuropharmacology. 2017 Dec;127:109-115. doi: 10.1016/j.neuropharm.2016.10.016.
82. Vetter I, Lewis RJ. Therapeutic potential of cone snail venom peptides (conopeptides). Curr Top Med Chem. 2012;12(14):1546-52. doi: 10.2174/156802612802652457.
83. Zhou M, Yang M, Wen H, Xu S, Han C, Wu Y. O1-conotoxin Tx6.7 cloned from the genomic DNA of Conus textile that inhibits calcium currents. J Venom Anim Toxins incl Trop Dis. 2023 May 22;29:e20220085. doi: 10.1590/1678–9199–JVATITD–2022–0085.
84. Sousa SR, McArthur JR, Brust A, Bhola RF, Rosengren KJ, Ragnarsson L, Dutertre S, Alewood PF, Christie MJ, Adams DJ, Vetter I, Lewis RJ. Novel analgesic ω-conotoxins from the vermivorous cone snail Conus moncuri provide new insights into the evolution of conopeptides. Sci Rep. 2018 Sep 7;8(1):13397. doi: 10.1038/s41598–018–31245–4.
85. Wang D, Himaya SWA, Giacomotto J, Hasan MM, Cardoso FC, Ragnarsson L, Lewis RJ. Characterisation of δ-Conotoxin TxVIA as a Mammalian T-Type Calcium Channel Modulator. Mar Drugs. 2020 Jun 30;18(7):343. doi: 10.3390/md18070343.
86. Kauferstein S, Huys I, Lamthanh H, Stöcklin R, Sotto F, Menez A, Tytgat J, Mebs D. A novel conotoxin inhibiting vertebrate voltage-sensitive potassium channels. Toxicon. 2003 Jul;42(1):43-52. doi: 10.1016/s0041–0101(03)00099–0.
87. Imperial JS, Bansal PS, Alewood PF, Daly NL, Craik DJ, Sporning A, Terlau H, López-Vera E, Bandyopadhyay PK, Olivera BM. A novel conotoxin inhibitor of Kv1.6 channel and nAChR subtypes defines a new superfamily of conotoxins. Biochemistry. 2006 Jul 11;45(27):8331-40. doi: 10.1021/bi060263r.
88. Naranjo D. Inhibition of single Shaker K channels by kappa-conotoxin-PVIIA. Biophys J. 2002 Jun;82(6):3003-11. doi: 10.1016/S0006–3495(02)75641–5.
89. Ferber M, Sporning A, Jeserich G, DeLaCruz R, Watkins M, Olivera BM, Terlau H. A novel conus peptide ligand for K+ channels. J Biol Chem. 2003 Jan 24;278(4):2177-83. doi: 10.1074/jbc.M205953200.
90. Chen P, Dendorfer A, Finol-Urdaneta RK, Terlau H, Olivera BM. Biochemical characterization of kappaM-RIIIJ, a Kv1.2 channel blocker: evaluation of cardioprotective effects of kappaM-conotoxins. J Biol Chem. 2010 May 14;285(20):14882-14889. doi: 10.1074/jbc.M109.068486.
91. Leipold E, Ullrich F, Thiele M, Tietze AA, Terlau H, Imhof D, Heinemann SH. Subtype-specific block of voltage-gated K+ channels by μ-conopeptides. Biochem Biophys Res Commun. 2017 Jan 22;482(4):1135-1140. doi: 10.1016/j.bbrc.2016.11.170.
92. Lazcano-Pérez F, Castro H, Arenas I, García DE, González-Muñoz R, Arreguín-Espinosa R. Activity of Palythoa caribaeorum Venom on Voltage-Gated Ion Channels in Mammalian Superior Cervical Ganglion Neurons. Toxins (Basel). 2016 May 5;8(5):135. doi: 10.3390/toxins8050135.
93. Díaz JM, Gracia AM, Cantera JR. Checklist of the Cone Shells (Mollusca: Gastropoda: Neogastropoda: Conidae) of Colombia. Biota Colomb. 2005;6(1):73–86.

94. Aguilar MB, Pérez-Reyes LI, López Z, de la Cotera EP, Falcón A, Ayala C, Galván M, Salvador C, Escobar LI. Peptide sr11a from Conus spurius is a novel peptide blocker for Kv1 potassium channels. Peptides. 2010 Jul;31(7):1287-91. doi: 10.1016/j.peptides.2010.04.007.
95. Bernáldez J, Jiménez S, González LJ, Ferro JN, Soto E, Salceda E, Chávez D, Aguilar MB, Licea-Navarro A. A New Member of Gamma-Conotoxin Family Isolated from Conus princeps Displays a Novel Molecular Target. Toxins (Basel). 2016 Feb 5;8(2):39. doi: 10.3390/toxins8020039.
96. Zamora-Bustillos R, Martínez-Núñez MA, Aguilar MB, Collí-Dula RC, Brito-Domínguez DA. Identification of Novel Conotoxin Precursors from the Cone Snail Conus spurius by High-Throughput RNA Sequencing. Mar Drugs. 2021 Sep 28;19(10):547. doi: 10.3390/md19100547.
97. Zamora-Bustillos R, Rivera-Reyes R, Aguilar MB, Michel-Morfín E, Landa-Jaime V, Falcón A, Heimer EP. Identification, by RT-PCR, of eight novel I_2-conotoxins from the worm-hunting cone snails Conus brunneus, Conus nux, and Conus princeps from the eastern Pacific (Mexico). Peptides. 2014 Mar;53:22-9. doi: 10.1016/j.peptides.2014.01.018.
98. Zugasti-Cruz A, Aguilar MB, Falcón A, Olivera BM, Heimer de la Cotera EP. Two new 4-Cys conotoxins (framework 14) of the vermivorous snail Conus austini from the Gulf of Mexico with activity in the central nervous system of mice. Peptides. 2008 Feb;29(2):179-85. doi: 10.1016/j.peptides.2007.09.021.
99. Bosmans F, Tytgat J. Voltage-gated sodium channel modulation by scorpion alpha-toxins. Toxicon. 2007 Feb;49(2):142-58. doi: 10.1016/j.toxicon.2006.09.023.
100. Olamendi-Portugal T, García BI, López-González I, Van Der Walt J, Dyason K, Ulens C, Tytgat J, Felix R, Darszon A, Possani LD. Two new scorpion toxins that target voltage-gated Ca2+ and Na+ channels. Biochem Biophys Res Commun. 2002 Dec 13;299(4):562-8. doi: 10.1016/s0006–291x(02)02706–7.
101. Beltrán-Vidal J, Carcamo-Noriega E, Pastor N, Zamudio-Zuñiga F, Guerrero-Vargas JA, Castaño S, Possani LD, Restano-Cassulini R. Colombian Scorpion Centruroides margaritatus: Purification and Characterization of a Gamma Potassium Toxin with Full-Block Activity on the hERG1 Channel. Toxins (Basel). 2021 Jun 8;13(6):407. doi: 10.3390/toxins13060407.
102. Gurrola GB, Rosati B, Rocchetti M, Pimienta G, Zaza A, Arcangeli A, Olivotto M, Possani LD, Wanke E. A toxin to nervous, cardiac, and endocrine ERG K+ channels isolated from Centruroides noxius scorpion venom. FASEB J. 1999 May;13(8):953-62.
103. DeBin JA, Maggio JE, Strichartz GR. Purification and characterization of chlorotoxin, a chloride channel ligand from the venom of the scorpion. Am J Physiol. 1993 Feb;264(2 Pt 1):C361-9. doi: 10.1152/ajpcell.1993.264.2.C361.
104. Sidach SS, Mintz IM. Kurtoxin, a gating modifier of neuronal high- and low-threshold ca channels. J Neurosci. 2002 Mar 15;22(6):2023-34. doi: 10.1523/JNEUROSCI.22–06–02023.2002.
105. Zhu HL, Wassall RD, Cunnane TC, Teramoto N. Actions of kurtoxin on tetrodotoxin-sensitive voltage-gated Na+ currents, NaV1.6, in murine vas deferens myocytes. Naunyn Schmiedebergs Arch Pharmacol. 2009 May;379(5):453-60. doi: 10.1007/s00210–008–0385–5.
106. Banerjee A, Lee A, Campbell E, Mackinnon R. Structure of a pore-blocking toxin in complex with a eukaryotic voltage-dependent K(+) channel. Elife. 2013 May 21;2:e00594. doi: 10.7554/eLife.00594.
107. Gao YD, Garcia ML. Interaction of agitoxin2, charybdotoxin, and iberiotoxin with potassium channels: selectivity between voltage-gated and Maxi-K channels. Proteins. 2003 Aug 1;52(2):146-54. doi: 10.1002/prot.10341.
108. Garcia ML, Knaus HG, Munujos P, Slaughter RS, Kaczorowski GJ. Charybdotoxin and its effects on potassium channels. Am J Physiol. 1995 Jul;269(1 Pt 1):C1-10. doi: 10.1152/ajpcell.1995.269.1.C1.
109. Feng J, Yu C, Wang M, Li Z, Wu Y, Cao Z, Li W, He X, Han S. Expression and characterization of a novel scorpine-like peptide Ev37, from the scorpion Euscorpiops validus. Protein Expr Purif. 2013 Mar;88(1):127-33. doi: 10.1016/j.pep.2012.12.004.
110. Bartok A, Toth A, Somodi S, Szanto TG, Hajdu P, Panyi G, Varga Z. Margatoxin is a non-selective inhibitor of human Kv1.3 K+ channels. Toxicon. 2014 Sep;87:6-16. doi: 10.1016/j.toxicon.2014.05.002.
111. Peigneur S, Esaki N, Yamaguchi Y, Tytgat J, Sato K. Effects of deletion and insertion of amino acids on the activity of HelaTx1, a scorpion toxin on potassium channels. Toxicon. 2016 Mar 1;111:1-5. doi: 10.1016/j.toxicon.2015.12.014.
112. Romi-Lebrun R, Lebrun B, Martin-Eauclaire MF, Ishiguro M, Escoubas P, Wu FQ, Hisada M, Pongs O, Nakajima T. Purification, characterization, and synthesis of three novel toxins from the Chinese scorpion Buthus martensi, which act on K+ channels. Biochemistry. 1997 Nov 4;36(44):13473-82. doi: 10.1021/bi971044w.
113. Landoulsi Z, Miceli F, Palmese A, Amoresano A, Marino G, El Ayeb M, Taglialatela M, Benkhalifa R. Subtype-selective activation of K(v)7 channels by AaTXKβ_{2-64}, a novel toxin variant from the Androctonus australis scorpion venom. Mol Pharmacol. 2013 Nov;84(5):763-73. doi: 10.1124/mol.113.088971.
114. Zoukimian C, Meudal H, De Waard S, Ouares KA, Nicolas S, Canepari M, Béroud R, Landon C, De Waard M, Boturyn D. Synthesis by native chemical ligation and characterization of the scorpion toxin AmmTx3. Bioorg Med Chem. 2019 Jan 1;27(1):247-253. doi: 10.1016/j.bmc.2018.12.009.
115. Teruel R, Roncallo CA. Rare or poorly known scorpions from Colombia. III. On the taxonomy and distribution of Rhopalurus laticauda Thorell, 1876 (*Scorpiones:* Buthidae), with description of a new species of the genus. Euscorpius. 2008;68:1–12. doi: 10.18590/euscorpius.2008.vol2008.iss68.1.
116. Carbone E, Wanke E, Prestipino G, Possani LD, Maelicke A. Selective blockage of voltage-dependent K+ channels by a novel scorpion toxin. Nature. 1982 Mar 4;296(5852):90-1. doi: 10.1038/296090a0.
117. Péter Jr M, Varga Z, Panyi G, Bene L, Damjanovich S, Pieri C, Possani LD, Gáspár R Jr. Pandinus imperator scorpion venom blocks voltage-gated K+ channels in human lymphocytes. Biochem Biophys Res Commun. 1998 Jan 26;242(3):621-5. doi: 10.1006/bbrc.1997.8018.
118. Batista CV, Gómez-Lagunas F, Rodríguez de la Vega RC, Hajdu P, Panyi G, Gáspár R, Possani LD. Two novel toxins from the Amazonian scorpion Tityus cambridgei that block Kv1.3 and Shaker B K(+)-channels with distinctly different affinities. Biochim Biophys Acta. 2002 Dec 16;1601(2):123-31. doi: 10.1016/s1570–9639(02)00458–2.
119. Bagdáany M, Batista CVF, Valdez-Cruz NA, Somodi S, de la Vega RCR, Licea AF, et al. Anuroctoxin, a New Scorpion Toxin of the α-KTx 6 Subfamily, Is Highly Selective for Kv1.3 over IKCa1 Ion Channels of Human T Lymphocytes. Mol Pharmacol. 2005;67:1034–44.
120. Cerni FA, Pucca MB, Amorim FG, de Castro Figueiredo Bordon K, Echterbille J, Quinton L, De Pauw E, Peigneur S, Tytgat J, Arantes EC. Isolation and characterization of Ts19 Fragment II, a new long-chain potassium channel toxin from Tityus serrulatus venom. Peptides. 2016 Jun;80:9-17. doi: 10.1016/j.peptides.2015.06.004.
121. Schwartz EF, Bartok A, Schwartz CA, Papp F, Gómez-Lagunas F, Panyi G, Possani LD. OcyKTx2, a new K^+-channel toxin characterized from the venom of the scorpion Opisthacanthus cayaporum. Peptides. 2013 Aug;46:40-6. doi: 10.1016/j.peptides.2013.04.021.
122. Rodríguez-Ravelo R, Restano-Cassulini R, Zamudio FZ, Coronas FI, Espinosa-López G, Possani LD. A K^+ channel blocking peptide from the Cuban scorpion Rhopalurus garridoi. Peptides. 2014 Mar;53:42-7. doi: 10.1016/j.peptides.2013.10.010.
123. Diego-García E, Abdel-Mottaleb Y, Schwartz EF, de la Vega RC, Tytgat J, Possani LD. Cytolytic and K+ channel blocking activities of beta-KTx and scorpine-like peptides purified from scorpion venoms. Cell Mol Life Sci. 2008 Jan;65(1):187-200. doi: 10.1007/s00018–007–7370–x.
124. Naseem MU, Gurrola-Briones G, Romero-Imbachi MR, Borrego J, Carcamo-Noriega E, Beltrán-Vidal J, Zamudio FZ, Shakeel K, Possani LD, Panyi G. Characterization and Chemical Synthesis of Cm39 (α-KTx 4.8): A Scorpion Toxin That Inhibits Voltage-Gated K+ Channel KV1.2 and Small- and Intermediate-Conductance Ca2+-Activated K+ Channels KCa2.2 and KCa3.1. Toxins (Basel). 2023 Jan 5;15(1):41. doi: 10.3390/toxins15010041.
125. Naseem MU, Carcamo-Noriega E, Beltrán-Vidal J, Borrego J, Szanto TG, Zamudio FZ, Delgado-Prudencio G, Possani LD, Panyi G. Cm28, a scorpion toxin having a unique primary structure, inhibits KV1.2 and KV1.3 with high affinity. J Gen Physiol. 2022 Aug 1;154(8):e202213146. doi: 10.1085/jgp.202213146.

126. Oliveira IS, Ferreira IG, Alexandre-Silva GM, Cerni FA, Cremonez CM, Arantes EC, Zottich U, Pucca MB. Scorpion toxins targeting Kv1.3 channels: insights into immunosuppression. J Venom Anim Toxins incl Trop Dis. 2019 Apr 15;25:e148118. doi: 10.1590/1678–9199–JVATITD–1481–18.
127. Restano-Cassulini R, Olamendi-Portugal T, Zamudio F, Becerril B, Possani LD. Two novel ergtoxins, blockers of K+-channels, purified from the Mexican scorpion Centruroides elegans elegans. Neurochem Res. 2008 Aug;33(8):1525-33. doi: 10.1007/s11064–008–9634–8.
128. Romero-Imbachi MR, Cupitra N, Ángel K, González B, Estrada O, Calderón JC, Guerrero-Vargas J, Beltrán J, Narvaez-Sanchez R. Centruroides margaritatus scorpion complete venom exerts cardiovascular effects through alpha-1 adrenergic receptors. Comp Biochem Physiol C Toxicol Pharmacol. 2021 Feb;240:108939. doi: 10.1016/j.cbpc.2020.108939.
129. D'Suze G, Batista CV, Frau A, Murgia AR, Zamudio FZ, Sevcik C, Possani LD, Prestipino G. Discrepin, a new peptide of the sub-family alpha-ktx15, isolated from the scorpion Tityus discrepans irreversibly blocks K+ -channels (IA currents) of cerebellum granular cells. Arch Biochem Biophys. 2004 Oct 15;430(2):256-63. doi: 10.1016/j.abb.2004.07.010.
130. Montero-Domínguez PA, Mares-Sámano S, Garduño-Juárez R. Insight on the interaction between the scorpion toxin blocker Discrepin on potassium voltage-gated channel Kv4.3 by molecular dynamics simulations. J Biomol Struct Dyn. 2023 Aug-Sep;41(13):6272-6281. doi: 10.1080/07391102.2022.2106514.
131. Picco C, Corzo G, Possani LD, Prestipino G. Interaction of the scorpion toxin discrepin with Kv4.3 channels and A-type K(+) channels in cerebellum granular cells. Biochim Biophys Acta. 2014 Sep;1840(9):2744-51. doi: 10.1016/j.bbagen.2014.05.009.
132. Adams ME. Agatoxins: ion channel specific toxins from the American funnel web spider, Agelenopsis aperta. Toxicon. 2004 Apr;43(5):509-25. doi: 10.1016/j.toxicon.2004.02.004.
133. Newcomb R, Szoke B, Palma A, Wang G, Chen Xh, Hopkins W, Cong R, Miller J, Urge L, Tarczy-Hornoch K, et al. Selective peptide antagonist of the class E calcium channel from the venom of the tarantula Hysterocrates gigas. Biochemistry. 1998 Nov 3;37(44):15353-62. doi: 10.1021/bi981255g.
134. Sutton KG, Siok C, Stea A, Zamponi GW, Heck SD, Volkmann RA, Ahlijanian MK, Snutch TP. Inhibition of neuronal calcium channels by a novel peptide spider toxin, DW13.3. Mol Pharmacol. 1998 Aug;54(2):407-18. doi: 10.1124/mol.54.2.407.
135. Liu Z, Dai J, Dai L, Deng M, Hu Z, Hu W, Liang S. Function and solution structure of Huwentoxin-X, a specific blocker of N-type calcium channels, from the Chinese bird spider Ornithoctonus huwena. J Biol Chem. 2006 Mar 31;281(13):8628-35. doi: 10.1074/jbc.M513542200.
136. McDonough SI, Lampe RA, Keith RA, Bean BP. Voltage-dependent inhibition of N- and P-type calcium channels by the peptide toxin omega-grammotoxin-SIA. Mol Pharmacol. 1997 Dec;52(6):1095-104. doi: 10.1124/mol.52.6.1095.
137. Fisyunov A, Pluzhnikov K, Molyavka A, Grishin E, Lozovaya N, Krishtal O. Novel spider toxin slows down the activation kinetics of P-type Ca2+ channels in Purkinje neurons of rat. Toxicology. 2005 Feb 1;207(1):129-36. doi: 10.1016/j.tox.2004.09.005.
138. Zarayskiy VV, Balasubramanian G, Bondarenko VE, Morales MJ. Heteropoda toxin 2 is a gating modifier toxin specific for voltage-gated K+ channels of the Kv4 family. Toxicon. 2005 Mar 15;45(4):431-42. doi: 10.1016/j.toxicon.2004.11.015.
139. Zeng X, Deng M, Lin Y, Yuan C, Pi J, Liang S. Isolation and characterization of Jingzhaotoxin-V, a novel neurotoxin from the venom of the spider Chilobrachys jingzhao. Toxicon. 2007 Mar 1;49(3):388-99. doi: 10.1016/j.toxicon.2006.10.012.
140. Diochot S, Drici MD, Moinier D, Fink M, Lazdunski M. Effects of phrixotoxins on the Kv4 family of potassium channels and implications for the role of Ito1 in cardiac electrogenesis. Br J Pharmacol. 1999 Jan;126(1):251-63. doi: 10.1038/sj.bjp.0702283.
141. Bertani R, Fukushima CS, Da Silva Jr PI. Two new species of Pamphobeteus pocock 1901 (*Araneae:* Mygalomorphae: Theraphosidae) from Brazil, with a new type of stridulatory organ. Zootaxa. 2008 Jul 21;1826:45–58. doi: 10.11646/zootaxa.1826.1.3.
142. Vásquez-Escobar J, Romero-Gutiérrez T, Morales JA, Clement HC, Corzo GA, Benjumea DM, Corrales-García LL. Transcriptomic Analysis of the Venom Gland and Enzymatic Characterization of the Venom of Phoneutria depilata (Ctenidae) from Colombia. Toxins (Basel). 2022 Apr 21;14(5):295. doi: 10.3390/toxins14050295.
143. Estrada-Gomez S, Vargas Muñoz LJ, Quintana Castillo JC. Extraction and partial characterization of venom from the Colombian spider Pamphobeteus aff. nigricolor (Aranae:Theraphosidae). Toxicon. 2013 Dec 15;76:301-9. doi: 10.1016/j.toxicon.2013.10.014.
144. Estrada-Gomez S, Muñoz LJ, Lanchero P, Latorre CS. Partial Characterization of Venom from the Colombian Spider Phoneutria Boliviensis (Aranae:Ctenidae). Toxins (Basel). 2015 Jul 31;7(8):2872-87. doi: 10.3390/toxins7082872.
145. Kalapothakis E, Penaforte CL, Leão RM, Cruz JS, Prado VF, Cordeiro MN, Diniz CR, Romano-Silva MA, Prado MA, Gomez MV, Beirão PS. Cloning, cDNA sequence analysis and patch clamp studies of a toxin from the venom of the armed spider (Phoneutria nigriventer). Toxicon. 1998 Dec;36(12):1971-80. doi: 10.1016/s0041–0101(98)00127–5.
146. Lúcio AD, Campos FV, Richardson M, Cordeiro MN, Mazzoni MS, de Lima ME, Pimenta MC, Bemquerer MP, Figueiredo SG, Gomes PC, Beirão PS. A new family of small (4kDa) neurotoxins from the venoms of spiders of the genus Phoneutria. Protein Pept Lett. 2008;15(7):700-8. doi: 10.2174/092986608785133708.
147. Cifuentes Y, Estrada-Gomez S, Vargas-Muñoz LJ, Perafán C. Description and molecular characterization of a new species of tarantula, *Pamphobeteus verdolaga*, from Colombia (Araneae: Mygalomorphae: Theraphosidae). Zoologia (Curitiba). 2016;33(6):e20160113. doi: 10.1590/s1984–4689zool–20160113.
148. Salinas-Restrepo C, Misas E, Estrada-Gómez S, Quintana-Castillo JC, Guzman F, Calderón JC, Giraldo MA, Segura C. Improving the Annotation of the Venom Gland Transcriptome of Pamphobeteus verdolaga, Prospecting Novel Bioactive Peptides. Toxins (Basel). 2022 Jun 15;14(6):408. doi: 10.3390/toxins14060408.
149. Salinas-Restrepo C, Naranjo-Duran AM, Quintana J, Bueno J, Guzman F, Hoyos Palacio LM, Segura C. Short Antimicrobial Peptide Derived from the Venom Gland Transcriptome of Pamphobeteus verdolaga Increases Gentamicin Susceptibility of Multidrug-Resistant Klebsiella pneumoniae. Antibiotics (Basel). 2023 Dec 20;13(1):6. doi: 10.3390/antibiotics13010006.
150. Estrada-Gomez S, Cardoso FC, Vargas-Muñoz LJ, Quintana-Castillo JC, Arenas Gómez CM, Pineda SS, Saldarriaga-Cordoba MM. Venomic, Transcriptomic, and Bioactivity Analyses of Pamphobeteus verdolaga Venom Reveal Complex Disulfide-Rich Peptides That Modulate Calcium Channels. Toxins (Basel). 2019 Aug 27;11(9):496. doi: 10.3390/toxins11090496.
151. Rojas-Palomino J, Gómez-Restrepo A, Giraldo MA, Calderón JC. Three new toxins from the south American spider *Pamphobeteus verdolaga* inhibit calcium and potassium channel currents of murine cardiomyocytes. Biophys J. 2024 Feb;123:264a. doi: 10.1016/j.bpj.2023.11.1655.
152. Martínez L, Sánchez-Ruiz A, Bonaldo AB. The spider genus Medionops Sánchez-Ruiz & Brescovit (*Araneae:* Caponiidae) in Colombia, with the description of four new species. Eur J Taxon. 2021;773:61–79. doi: 10.5852/ejt.2021.773.1511.
153. de Weille JR, Schweitz H, Maes P, Tartar A, Lazdunski M. Calciseptine, a peptide isolated from black mamba venom, is a specific blocker of the L-type calcium channel. Proc Natl Acad Sci U S A. 1991 Mar 15;88(6):2437-40. doi: 10.1073/pnas.88.6.2437.
154. Zhang P, Shi J, Shen B, Li X, Gao Y, Zhu Z, Zhu Z, Ji Y, Teng M, Niu L. Stejnihagin, a novel snake metalloproteinase from Trimeresurus stejnegeri venom, inhibited L-type Ca2+ channels. Toxicon. 2009 Feb;53(2):309-15. doi: 10.1016/j.toxicon.2008.12.006.
155. Robertson B, Owen D, Stow J, Butler C, Newland C. Novel effects of dendrotoxin homologues on subtypes of mammalian Kv1 potassium channels expressed in Xenopus oocytes. FEBS Lett. 1996 Mar 25;383(1-2):26-30. doi: 10.1016/0014–5793(96)00211–6.
156. Yang W, Feng J, Wang B, Cao Z, Li W, Wu Y, Chen Z. BF9, the first functionally characterized snake toxin peptide with Kunitz-type protease and potassium channel inhibiting properties. J Biochem Mol Toxicol. 2014 Feb;28(2):76-83. doi: 10.1002/jbt.21538.

157. Kleiz-Ferreira JM, Bernaerts H, Pinheiro-Junior EL, Peigneur S, Zingali RB, Tytgat J. Pharmacological Screening of Venoms from Five Brazilian Micrurus Species on Different Ion Channels. Int J Mol Sci. 2022 Jul 13;23(14):7714. doi: 10.3390/ijms23147714.
158. Triplitt C, Chiquette E. Exenatide: from the Gila monster to the pharmacy. J Am Pharm Assoc (2003). 2006 Jan-Feb;46(1):44-52; quiz 53-5. doi: 10.1331/154434506775268698.
159. MacDonald PE, Salapatek AM, Wheeler MB. Glucagon-like peptide-1 receptor activation antagonizes voltage-dependent repolarizing K(+) currents in beta-cells: a possible glucose-dependent insulinotropic mechanism. Diabetes. 2002 Dec;51 Suppl 3:S443-7. doi: 10.2337/diabetes.51.2007.s443.
160. Wang YC, Wang L, Shao YQ, Weng SJ, Yang XL, Zhong YM. Exendin-4 promotes retinal ganglion cell survival and function by inhibiting calcium channels in experimental diabetes. iScience. 2023 Aug 18;26(9):107680. doi: 10.1016/j.isci.2023.107680.
161. Mueller P, Rudin DO, Tien HT, Wescott WC. Reconstitution of cell membrane structure in vitro and its transformation into an excitable system. Nature. 1962 Jun 9;194:979-80. doi: 10.1038/194979a0.
162. Thompson TE. Experimental bilayer membrane models. Protoplasma. 1967;63(1):194-6.
163. Tobias JM, Agin DP, Pawlowski R. The excitable system in the cell surface. Circulation. 1962 Nov;26:1145-50. doi: 10.1161/01.cir.26.5.1145. PMID: 13985211.
164. Kennedy SJ, Roeske RW, Freeman AR, Watanabe AM, Besche HR Jr. Synthetic peptides form ion channels in artificial lipid bilayer membranes. Science. 1977 Jun 17;196(4296):1341-2. doi: 10.1126/science.867034.
165. Chanturiya AN, Nikoloshina HV. Correlations between changes in membrane capacitance induced by changes in ionic environment and the conductance of channels incorporated into bilayer lipid membranes. J Membr Biol. 1994 Jan;137(1):71-7. doi: 10.1007/BF00234999.
166. Priyadarshini D, Ivica J, Separovic F, de Planque MRR. Characterisation of cell membrane interaction mechanisms of antimicrobial peptides by electrical bilayer recording. Biophys Chem. 2022 Feb;281:106721. doi: 10.1016/j.bpc.2021.106721.
167. Sharma G, Deuis JR, Jia X, Mueller A, Vetter I, Mobli M. Recombinant production, bioconjugation and membrane binding studies ofPn3a, a selective NaV1.7 inhibitor. Biochem Pharmacol. 2020 Nov;181:114148. doi: 10.1016/j.bcp.2020.114148.
168. Chen M, Blum D, Engelhard L, Raunser S, Wagner R, Gatsogiannis C. Molecular architecture of black widow spider neurotoxins. Nat Commun. 2021 Nov 29;12(1):6956. doi: 10.1038/s41467–021–26562–8.
169. Komiya M, Kato M, Tadaki D, Ma T, Yamamoto H, Tero R, Tozawa Y, Niwano M, Hirano-Iwata A. Advances in Artificial Cell Membrane Systems as a Platform for Reconstituting Ion Channels. Chem Rec. 2020 Jul;20(7):730-742. doi: 10.1002/tcr.201900094.
170. D'Suze G, Zamudio F, Gómez-Lagunas F, Possani LD. A novel K+ channel blocking toxin from Tityus discrepans scorpion venom. FEBS Lett. 1999 Jul 30;456(1):146-8. doi: 10.1016/s0014–5793(99)00947–3.
171. Woodcock EA, Matkovich SJ. Cardiomyocytes structure, function and associated pathologies. Int J Biochem Cell Biol. 2005 Sep;37(9):1746-51. doi: 10.1016/j.biocel.2005.04.011.
172. Liu J, Laksman Z, Backx PH. The electrophysiological development of cardiomyocytes. Adv Drug Deliv Rev. 2016 Jan 15;96:253-73. doi: 10.1016/j.addr.2015.12.023.
173. Walker CA, Spinale FG. The structure and function of the cardiac myocyte: a review of fundamental concepts. J Thorac Cardiovasc Surg. 1999 Aug;118(2):375-82. doi: 10.1016/S0022–5223(99)70233–3.
174. Yamakage M, Namiki A. Calcium channels--basic aspects of their structure, function and gene encoding; anesthetic action on the channels--a review. Can J Anaesth. 2002 Feb;49(2):151-64. doi: 10.1007/BF03020488.
175. Hussain M, Orchard CH. Sarcoplasmic reticulum Ca2+ content, L-type Ca2+ current and the Ca2+ transient in rat myocytes during beta-adrenergic stimulation. J Physiol. 1997 Dec 1;505 (Pt 2)(Pt 2):385-402. doi: 10.1111/j.1469–7793.1997.385bb.x.
176. Kumari N, Gaur H, Bhargava A. Cardiac voltage gated calcium channels and their regulation by β-adrenergic signaling. Life Sci. 2018 Feb 1;194:139-149. doi: 10.1016/j.lfs.2017.12.033.
177. Mewes T, Ravens U. L-type calcium currents of human myocytes from ventricle of non-failing and failing hearts and from atrium. J Mol Cell Cardiol. 1994 Oct;26(10):1307-20. doi: 10.1006/jmcc.1994.1149.
178. Chen L, Sampson KJ, Kass RS. Cardiac Delayed Rectifier Potassium Channels in Health and Disease. Card Electrophysiol Clin. 2016 Jun;8(2):307-22. doi: 10.1016/j.ccep.2016.01.004.
179. Grandi E, Sanguinetti MC, Bartos DC, Bers DM, Chen-Izu Y, Chiamvimonvat N, Colecraft HM, Delisle BP, Heijman J, Navedo MF, et al. Potassium channels in the heart: structure, function and regulation. J Physiol. 2017 Apr 1;595(7):2209-2228. doi: 10.1113/JP272864.
180. Bertaso F, Sharpe CC, Hendry BM, James AF. Expression of voltage-gated K+ channels in human atrium. Basic Res Cardiol. 2002 Nov;97(6):424-33. doi: 10.1007/s00395–002–0377–4.
181. Tamargo J, Caballero R, Gómez R, Valenzuela C, Delpón E. Pharmacology of cardiac potassium channels. Cardiovasc Res. 2004 Apr 1;62(1):9-33. doi: 10.1016/j.cardiores.2003.12.026.
182. Rush AM, Waxman S. Dorsal root ganglion Neurons. In: Squire LR, editor. Encyclopedia of Neuroscience. Academic Press; 2009. p. 615–9.
183. Marani E. Dorsal Root or spinal ganglion. Ref Modul Neurosci Biobehav Psychol. Elsevier; 2017. doi: 10.1016/B978–0–12–809324–5.04160–2.
184. Papka RE. Sensory Ganglia. In: Squire LR, editor. Encyclopedia of Neuroscience. Academic Press; 2009. p. 657–68.
185. Schmidt R, Gebhart G. Neurofilament Protein NF200. In: Gebhart G., Schmidt R., editors. Encyclopedia of Pain. Berlin, Heidelberg: Springer Berlin Heidelberg; 2013. p. 2046–2046.
186. Katsetos CD, Legido A, Perentes E, Mörk SJ. Class III beta-tubulin isotype: a key cytoskeletal protein at the crossroads of developmental neurobiology and tumor neuropathology. J Child Neurol. 2003 Dec;18(12):851-66; discussion 867. doi: 10.1177/088307380301801205.
187. Zuchero JB. Purification and culture of dorsal root ganglion neurons. Cold Spring Harb Protoc. 2014 Aug 1;2014(8):813-4. doi: 10.1101/pdb.top073965.
188. Villière V, McLachlan EM. Electrophysiological properties of neurons in intact rat dorsal root ganglia classified by conduction velocity and action potential duration. J Neurophysiol. 1996 Sep;76(3):1924-41. doi: 10.1152/jn.1996.76.3.1924.
189. Wang M, Guan X, Liang S. The cross channel activities of spider neurotoxin huwentoxin-I on rat dorsal root ganglion neurons. Biochem Biophys Res Commun. 2007 Jun 8;357(3):579-83. doi: 10.1016/j.bbrc.2007.02.168.
190. Diochot S, Schweitz H, Béress L, Lazdunski M. Sea anemone peptides with a specific blocking activity against the fast inactivating potassium channel Kv3.4. J Biol Chem. 1998 Mar 20;273(12):6744-9. doi: 10.1074/jbc.273.12.6744.
191. Trequattrini C, Zamudio FZ, Petris A, Prestipino G, Possani LD, Franciolini F. Tityus bahiensis toxin IV-5b selectively affects Na channel inactivation in chick dorsal root ganglion neurons. Comp Biochem Physiol A Physiol. 1995 Sep;112(1):21-8. doi: 10.1016/0300–9629(95)00096–p.
192. Roy ML, Narahashi T. Sodium channels of rat dorsal root ganglion neurons. In: Narahashi T, editor. Methods in Neurosciences. Academic Press; 1994. p. 21–38.
193. Royero P, García L, Rosales A, D'Suze G, Sevcik C, Castillo C. Bactridine 2 effect in DRG neurons. Identification of NHE as a second target. Toxicon. 2018 Sep 1;151:37-46. doi: 10.1016/j.toxicon.2018.06.083.
194. Tsantoulas C, McMahon SB. Opening paths to novel analgesics: the role of potassium channels in chronic pain. Trends Neurosci. 2014 Mar;37(3):146-58. doi: 10.1016/j.tins.2013.12.002.
195. Zemel BM, Ritter DM, Covarrubias M, Muqeem T. A-Type KV Channels in Dorsal Root Ganglion Neurons: Diversity, Function, and Dysfunction. Front Mol Neurosci. 2018 Aug 6;11:253. doi: 10.3389/fnmol.2018.00253.
196. Ackers-Johnson M, Foo RS. Langendorff-Free Isolation and Propagation of Adult Mouse Cardiomyocytes. Methods Mol Biol. 2019;1940:193-204. doi: 10.1007/978–1–4939–9086–3_14.

197. Bell RM, Mocanu MM, Yellon DM. Retrograde heart perfusion: the Langendorff technique of isolated heart perfusion. J Mol Cell Cardiol. 2011 Jun;50(6):940-50. doi: 10.1016/j.yjmcc.2011.02.018.

198. Li H, Liu C, Bao M, Liu W, Nie Y, Lian H, Hu S. Optimized Langendorff perfusion system for cardiomyocyte isolation in adult mouse heart. J Cell Mol Med. 2020 Dec;24(24):14619-14625. doi: 10.1111/jcmm.15773.

199. Lin YT, Chen JC. Dorsal Root Ganglia Isolation and Primary Culture to Study Neurotransmitter Release. J Vis Exp. 2018 Oct 6;(140):57569. doi: 10.3791/57569.

200. Kolb I, Stoy WA, Rousseau EB, Moody OA, Jenkins A, Forest CR. Cleaning patch-clamp pipettes for immediate reuse. Sci Rep. 2016 Oct 11;6:35001. doi: 10.1038/srep35001.

201. Lacampagne A, Duittoz A, Bolaños P, Peineau N, Argibay JA. Effect of sulfhydryl oxidation on ionic and gating currents associated with L-type calcium channels in isolated guinea-pig ventricular myocytes. Cardiovasc Res. 1995 Nov;30(5):799-806.

202. Escoubas P, Diochot S, Célérier ML, Nakajima T, Lazdunski M. Novel tarantula toxins for subtypes of voltage-dependent potassium channels in the Kv2 and Kv4 subfamilies. Mol Pharmacol. 2002 Jul;62(1):48-57. doi: 10.1124/mol.62.1.48.

203. Kubista H, Mafra RA, Chong Y, Nicholson GM, Beirão PS, Cruz JS, Boehm S, Nentwig W, Kuhn-Nentwig L. CSTX-1, a toxin from the venom of the hunting spider Cupiennius salei, is a selective blocker of L-type calcium channels in mammalian neurons. Neuropharmacology. 2007 Jun;52(8):1650-62. doi: 10.1016/j.neuropharm.2007.03.012.

204. Nesher N, Zlotkin E, Hochner B. The sea anemone toxin AdE-1 modifies both sodium and potassium currents of rat cardiomyocytes. Biochem J. 2014 Jul 1;461(1):51-9. doi: 10.1042/BJ20131454.

205. Orts DJ, Peigneur S, Silva-Gonçalves LC, Arcisio-Miranda M, P W Bicudo JE, Tytgat J. AbeTx1 Is a Novel Sea Anemone Toxin with a Dual Mechanism of Action on Shaker-Type K^+ Channels Activation. Mar Drugs. 2018 Oct 1;16(10):360. doi: 10.3390/md16100360.

206. Xia J, Wright J, Adams CE. Five large Chinese biomedical bibliographic databases: accessibility and coverage. Health Info Libr J. 2008 Mar;25(1):55-61. doi: 10.1111/j.1471–1842.2007.00734.x.

207. Lai MC, Wu SN, Huang CW. The Specific Effects of OD-1, a Peptide Activator, on Voltage-Gated Sodium Current and Seizure Susceptibility. Int J Mol Sci. 2020 Nov 4;21(21):8254. doi: 10.3390/ijms21218254.